Nazarbayev University School of Engineering and Digital Sciences Chemical and Materials Engineering Department ENG 400 Capstone Project I

Report 4

Design of Plant for Industrial Production of Styrene

Group members:

Tangsulu Adil 202112675

Zhaniya Askar 201942562

Kazbek Kulbergenov 202093434

Tanay Umurzak 202117615

Orazaly Sultan-Akhmetov 202055612

Instructor: Professor Dhawal Shah

Supervisors: Professor Stavros Poulopoulos

Professor Yanwei Wang

Spring 2025

Astana, Kazakhstan

Date: 20th April, 2025

Work Distribution

Chapter	Assigned Task	Orazaly	Tangsulu	Tanay	Zhaniya	Kazbek
1	**Process Introduction**					
1.1	General Physical and Chemical Properties of Styrene				**1st**	
1.2	Styrene Applications and Production Rate				**1st**	
1.3	Preliminary Market Analysis				**1st**	
1.4	Preliminary Economic Analysis				**1st**	
2	**Process Summary**			**1st**		
3	**Major Component Design**					
3.1	HEX-101 heat exchanger design				**1st**	
3.2	R-101 and R-102 Reactors design	**1st**				
3.3	C-101 Three-Phase Separator					**1st**
3.4	DC-101 Distillation column design			**1st**		
3.5	DC-102 Vacuum distillation column		**1st**			
4	**Minor Equipment Design**					
4.1	Pump design				**1st**	
4.2	Heaters, coolers, boiler design	**1st**				
4.3	Compressor design			**1st**		
4.4	Storage tank design		**1st**			
5	**Plant Location and Layout**					
5.1	Plant site location	**1st**				
5.2	Plan layout	**1st**				

6	**Environmental and Waste Streams**					**1st**
7	**Total Investment and Profitability**					
7.1	Price of Raw Material, Consumable and Final Product		**1st**			
7.2	Cost of Equipments		**1st**			
7.3	Capital Investment Estimation		**1st**			
7.4	Fixed Operating Cost of Production		**1st**			
7.5	Variable Cost of Production		**1st**			
7.6	Economic Analysis		**1st**			
8	**Conclusion and Future Work**				**1st**	

Table of Contents

List of Abbreviations

ABS	Acrylonitrile butadiene styrene
BAT	Best Available Technique
BZ	Benzene
CAGR	Compound annual growth rate
CC	Contingency cost
CIS	Commonwealth of Independent States
EAEU	Eurasian Economic Union
EB	Ethylbenzene
EBHP	Ethylbenzene hydroperoxide
EPS	Expanded Polystyrene
ISBL	Inside Battery Limits
EC	Engineering cost
ET	Ethylene
H2O	Water
IARC	International Agency for Research on Cancer
MBA	Methylbenzyl alcohol
MT	Methane
NPV	Net Present Value
NRTL	Non-random two-liquid
OSBL	Outside battery limits
ODH	Oxidative dehydrogenation
PFR	Process flow diagrams
POSM	Propylene oxide–styrene monomer
PS	Polystyrene
SBR	Styrene-butadiene rubber
ST	Styrene
USD	United States Dollar
KZT	Tenge

Chapter 1: Process Introduction

Styrene is a fundamental monomer in the modern petrochemical industry, widely used in the production of materials such as polystyrene (PS), acrylonitrile butadiene styrene (ABS), and styrene-butadiene rubber (SBR) [1, 2]. These polymers play a crucial role in packaging, automotive parts, electronics, and the construction sector due to their mechanical robustness and lightweight properties [3, 4]. The styrene's versatility, coupled with global demand for durable and recyclable plastics, highlights the importance of establishing local production capabilities.

Kazakhstan possesses the strategic potential to become a regional hub for styrene manufacturing. With abundant reserves of crude oil and natural gas - the upstream sources for ethylene (ET) and benzene (BZ) used to produce ethylbenzene (EB), the immediate precursor of styrene - the country is well-positioned to support a vertically integrated supply chain [5, 6]. Supported by government policies and investments totaling 194.4 billion KZT in 2023, Kazakhstan's chemical industry saw the launch of 14 industrial projects worth over 29 billion KZT in 2024, reflecting a favorable environment for petrochemical expansion [7, 8].

Kazakhstan's geographic placement within the Eurasian Economic Union (EAEU) provides additional logistical advantages. Through tariff-free trade and access to developing CIS markets, such as Russia, Armenia, and Kyrgyzstan, locally produced styrene could serve both domestic and export demand efficiently [9, 10].

This project aims to design a cost-effective and scalable styrene production facility using the dehydrogenation of ethylbenzene as the primary route [11]. This method is globally dominant and offers high selectivity and yield, aligning with Kazakhstan's industrial capacity, feedstock availability, and regional market dynamics.

1.1. General Physical and Chemical Properties of Styrene

Styrene (ST), with the chemical formula $CH_2=CHC_6H_5$, is a vinyl aromatic compound [1]. Its structure consists of a benzene ring (C_6H_5) attached to a vinyl group ($CH=CH_2$), making it highly reactive and prone to polymerization [2]. This double bond in the vinyl group allows styrene to form long polymer chains under the right conditions, making it ideal for producing

materials such as PS and ABS plastics. The styrene's physicochemical properties are shown in Table 1.1.

Table 1.1. Key Physical Properties [12].

Property	**Styrene**
Chemical Formula	C_8H_8
Structural Formula	$CH_2{=}CHC_6H_5$
Molecular Weight	104.15 g/mol
Boiling Point	145 °C (293°F)
Freezing Point	-30.63°C (-23.1°F)
Specific Density	0.905 g/cm³ at 25°C
Odor	Sweet, penetrating smell
Solubility	Insoluble in water

Due to its widespread industrial use, styrene has been evaluated for health and environmental risks. The International Agency for Research on Cancer (IARC) classifies it as a Group 2B compound, indicating it is possibly carcinogenic to humans [13]. As a result, industrial operations involving styrene must adopt stringent safety measures such as containment systems, proper ventilation, and regular monitoring of occupational exposure. Additional toxicological effects are provided in Appendix A1 [13].

1.2. Styrene Applications and Production Rate

Styrene production can follow several industrial routes, including catalytic dehydrogenation of ethylbenzene, oxidative dehydrogenation (ODH), and co-production via the propylene oxide–styrene monomer (POSM) process. Among these, catalytic dehydrogenation of ethylbenzene is the most established method, accounting for approximately 85–90% of global styrene production [13, 14].

This endothermic and reversible reaction is typically conducted in the vapor phase at 600–650 °C using a potassium-promoted iron oxide catalyst [3, 4, 14]. The principal reaction proceeds as follows (Equation 1.1):

$$C_6H_5CH_2CH_3 \Leftrightarrow CH_2{=}CHC_6H_5 + H_2 \qquad (1.1)$$

During the primary reaction, certain components also engage in side reactions, leading to the formation of unwanted by-products:

Benzene and Ethylene Reaction is presented by the following Equation (1.2):

$$C_6H_5CH_2CH_3 \Rightarrow C_6H_6 + C_2H_4 \quad (1.2)$$

Toluene Reaction, shown in Equation (1.3):

$$CH_2{=}CHC_6H_5 + 2H_2 \Rightarrow C_6H_5CH_2CH_3 + CH_4 \quad (1.3)$$

To maximize styrene yield and selectivity, the process operates at low pressures and elevated temperatures. Steam is co-fed with ethylbenzene to serve as a heat carrier, reduce the partial pressures of reactants and products, and mitigate coke formation on the catalyst surface [14].

Alternative processes were evaluated for this project. The ODH route, while exothermic and not limited by equilibrium constraints, exhibits lower styrene selectivity and involves more complex purification due to the formation of carbon oxides [15]. The POSM process enables the co-production of valuable propylene oxide and achieves high purity, but it is capital-intensive and highly dependent on the parallel market demand for propylene oxide [16]. Further technical details and detailed comparison are provided in Appendix A2 [16, 17].

Given its high selectivity (94–97%), product purity exceeding 99%, and widespread industrial adoption, the catalytic dehydrogenation of ethylbenzene remains the preferred production route. This method also aligns well with Kazakhstan's domestic availability of benzene and ethylene feedstocks [5, 6], offering a technically and economically viable solution for local production.

1.3. Preliminary Market Analysis

The global demand for styrene has exhibited robust growth in recent years. In 2023, the global styrene market was valued at approximately USD 56.43 billion, and it is projected to reach USD 97.31 billion by 2032, corresponding to a compound annual growth rate (CAGR) of

6.24% [18]. This demand is fueled by styrene's widespread use in lightweight, durable materials across key industrial sectors [19].

Global production volume is rising in tandem with market value. In 2025, total styrene output is estimated at 36.27 million tonnes and is expected to reach 47.00 million tonnes by 2030 [20]. The Asia-Pacific region remains the dominant consumer, accounting for roughly 52% of global demand as of 2022 [19]. Notably, the CIS market is also expanding, with rising interest in domestic production to reduce reliance on imports. The Styrene Distribution market is illustrated in Appendix A3 [20]. Leading producers on the global stage include Chevron Phillips, Ineos, Shell, Alpek, and Nova Chemicals, which operate large-scale, vertically integrated facilities [21].

Catalytic dehydrogenation of ethylbenzene, predominant method for styrene production, itself is produced from benzene and ethylene—key intermediates derived from crude oil and natural gas [22]. The ethylbenzene market, tightly coupled with styrene demand, is forecasted to grow from 36.01 million tonnes in 2025 to 41.81 million tonnes by 2029 [23]. However, feedstock prices have shown considerable volatility in recent years: benzene prices surged in 2022 due to supply shortages, while ethylene prices dropped in 2023 amid global production adjustments [24, 25].

Regionally, Russia remains the sole ethylbenzene producer within the CIS, with an annual capacity of 450,000 tonnes distributed between Sibur-Khimprom and Gazprom Neftkhim Salavat facilities [26]. These plants utilize advanced zeolite-based catalysts, signaling a shift toward more energy-efficient and environmentally conscious technologies [27]. Given Kazakhstan's lack of domestic ethylbenzene production, these trends highlight a significant opportunity for local capacity building.

1.4. Preliminary Economic Analysis

Building upon the favorable market outlook, a preliminary economic assessment was conducted to evaluate the feasibility of establishing a styrene production facility in Kazakhstan. Based on projected regional consumption trends, a proposed plant capacity of 237.9 ktonnes per year was estimated to meet approximately 25% of the anticipated CIS demand by 2027. This

target was determined using global per capita styrene consumption data extrapolated to the combined population of CIS countries, ensuring both scalability and market relevance.

Given the absence of ethylbenzene production within Kazakhstan, the economic model assumes imports from China, priced at around USD 1,200 per tonne [28]. Despite this dependency, the estimated average market price for styrene—approximately USD 1,700 per tonne - suggests a potential gross revenue of USD 408.621 million annually for the proposed facility [29]. Revenue calculations are presented in ESI "Economic analysis". These projections incorporate conservative yield assumptions and reflect typical operating efficiencies for industrial dehydrogenation units.

Furthermore, the selection of Pavlodar as a production site introduces significant cost-saving advantages. Utility rates in the region are among the lowest in the country, with water priced at 95.19 KZT/m³ and electricity at 19.2 KZT/kWh - both substantially lower than in alternative industrial hubs such as Atyrau [30–33]. These favorable conditions, coupled with Pavlodar's proximity to key petrochemical infrastructure and logistical corridors, contribute to a strong economic case for investment.

The preliminary analysis thus confirms both market demand and economic viability, reinforcing the strategic rationale for local styrene production aligned with national industrialization goals and regional supply chain integration.

Chapter 2: Process Summary

The production of styrene from the hydrogenation of ethylbenzene consists of three main stages: production of hydrocarbons, three-phase separation, and purification of styrene. The process flow diagram for the production of targeted 99% mole styrene is displayed in the Figure 2.1

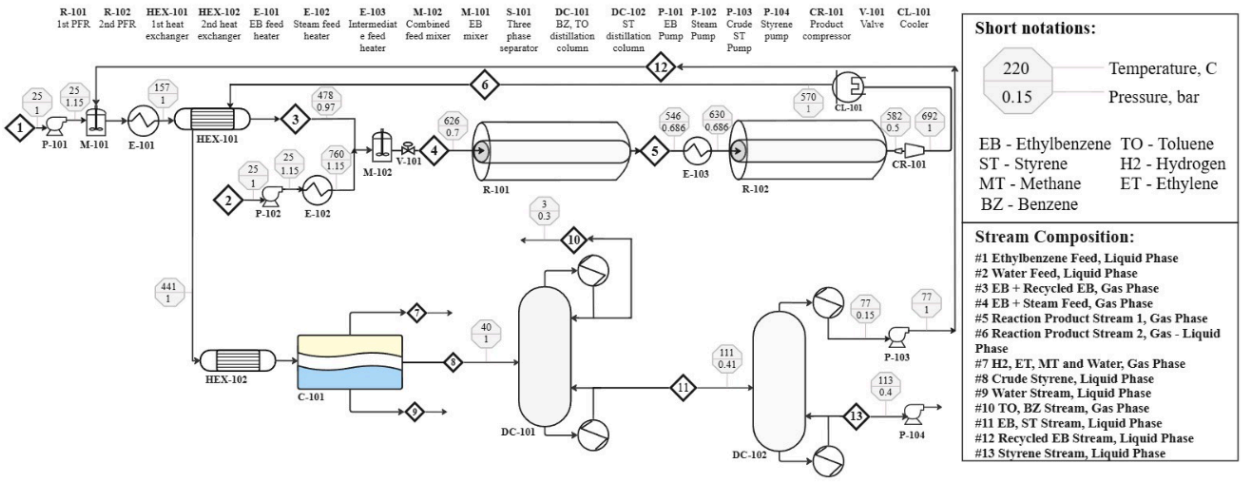

Figure 2.1. Process Flow Diagram of ST production.

2.1. Production of Hydrocarbons

In this stage, raw ethylbenzene, liquid water, and recycled ethylbenzene are introduced into the reactor system. Pure liquid ethylbenzene, designated as Stream 1, enters at 25 °C and 1 bar and combines in a mixer with recycled ethylbenzene, Stream 12, which is at 77 °C and 1 bar. The water feed, Stream 2, also at 25 °C and 1 bar, joins the ethylbenzene mixture before entering the first reactor. To meet the reactor's operational requirements, all streams undergo preheating.

Stream 1 is first processed through pump P-101, which increases its pressure to 1.15 bar to facilitate liquid flow from the storage tank. After mixing with recycled ethylbenzene in mixer M-101, the combined stream is heated to 627 °C using heater E-101 and heat exchanger HEX-101 in series, while its pressure adjusts to 0.7 bar. The hot fluid for HEX-101 is the effluent from the second plug flow reactor, R-102, at 692 °C and 1 bar. Meanwhile, the water feed, Stream 2, is pumped through P-102 from its feed tank and heated to 760 °C in heater E-102, achieving a state of 760 °C and 1.15 bar before entering mixer M-102.

The resulting mixed stream, Stream 4, at 627 °C and 0.7 bar, is fed into a series of plug flow reactors, R-101 and R-102. Both reactors operate at 630 °C, though their pressure conditions differ: R-101 at 0.7 bar and R-102 at 1.044 bar. After exiting the first reactor, Stream 5, which has cooled to 546 °C, is reheated to 630 °C by heater E-103 to maintain consistent

reaction conditions and maximize ethylbenzene conversion. The final product stream, Stream 6, containing styrene, unreacted ethylbenzene, and side hydrocarbons, exits the second reactor at 582 °C and 0.5 bar. The temperature decrease results from heat losses to the surroundings through conduction, convection, and radiation, while the pressure drop is attributed to frictional losses. The conditions and compositions of all streams in this stage are detailed in Table 2.1.

Table 2.1. Material balance results from the production of hydrocarbons.

Stream	**1**	**2**	**3**	**4**	**5**	**6**
Temperature °C	25	25	478	676	546	570
Pressure, bar	1	1	2.3	0.7	0.69	1
Phase	Liquid	Liquid	Vapor	Vapor	Vapor	Vapor
Components Mass Flow Rate						
Total, kg/h	31850.1	59449.5	45494.86	104944.36	104997.32	104997.19
EB	31850.1	0	44760.95	44760.95	26784.1	14200.88
ST	0	0	384.66	384.66	17483.85	28368.09
H2O	0	59449.5	0	59449.5	59449.5	59449.5
TO	0	0	349.2	349.2	649.89	1748.94
MT	0	0	0	0	113.14	304.46
ET	0	0	0	0	52.87	111.48
BZ	0	0	0.04	0.04	147.21	310.44
H2	0	0	0	0	316.76	503.4

2.2. Three-phase separation

Stream 6, exiting reactor R-102, flows into compressor CR-101, which raises its pressure to 1 bar and increases its temperature to 692 °C. This adjustment is essential to align with the operational requirements of the downstream three-phase separator, C-101, which separates Stream 6 into three distinct streams based on phase and composition. Prior to entering the C-101 separator, Stream 6 acts as the hot fluid in the HEX-101 heat exchanger. To meet the separator's operating conditions, the CL-101 cooler lowers the stream's temperature to 570 °C. After passing through the heat exchanger, the temperature further decreases, resulting in a feed to the C-101 separator at 440 °C and 1 bar. In the C-101 three-phase separator, Stream 6 is divided into three streams. The top stream, Stream 7, consists of hydrogen, methane, and ethylene in the gas phase

and is designated as a waste stream, removed from the process. The bottom stream, Stream 9, primarily liquid water, is also classified as a waste stream and is not utilized further in the process. The middle stream, Stream 8, containing styrene, unreacted ethylbenzene, benzene, and toluene, exits the separator at 60 °C and 1 bar and proceeds to the DC-101 distillation column for further processing. The conditions of all streams involved in this stage are detailed in Table 2.2, which provides comprehensive information on their temperature, pressure, and composition.

Table 2.2. Material balance results from the three-phase separation.

Stream	**7**	**8**	**9**
Temperature, °C	40	40	40
Pressure, bar	1	1	1
Phase	Vapor	Liquid	Liquid
Components Mass Flow Rate			
Total, kg/h	2118.18	43793.47	59085.55
EB	287.13	13863.98	49.77
ST	386.71	27979.42	1.96
H2O	401.88	38.64	59008.98
TO	89.54	1634.72	24.68
MT	304.45	0	0.01
ET	111.47	0	0.01
BZ	33.59	276.71	0.13
H2	0	0	0

2.3. Styrene purification

Stream 10, which is the distillate output from distillation column DC-101, primarily consists of toluene and benzene. These two components are challenging to separate effectively within the C-101 unit due to their similar volatilities. Meanwhile, the heavier mixture of styrene and ethylbenzene exits as the bottom product (Stream 11) from DC-101 and is subsequently directed to the final distillation unit, DC-102, for further separation.

DC-101 operates under specific conditions to optimize component separation: the reboiler functions at a temperature of 110 °C and a pressure of 0.41 bar, with a reflux ratio of 3.0.

The overhead condenser is maintained at 40.3 °C and 0.3 bar to facilitate efficient condensation of lighter components.

The final separation takes place in DC-102 with a reflux ratio of 16.34, where ethylbenzene is separated from styrene. Stream 13, which contains purified styrene at a molar purity of 99%, exits the bottom of DC-102 at 113 °C and 0.4 bar. This stream is then routed through pump P-104, which transfers it to the designated storage tank. The overhead product of DC-102, Stream 12, comprises the unreacted ethylbenzene and is recycled back into the process via mixer M-101. Representation of the stream conditions are displayed in Table 2.3.

Table 2.3. Materials balance results from the styrene purification.

Stream	**10**	**11**	**12**	**13**
Temperature, °C	40	111	77	113
Pressure, bar	0.3	0.41	1	0.4
Phase	Liquid	Liquid	Liquid	Liquid
Components Mass Flow Rate				
Total, kg/h	2709.71	41083.76	13644.76	27439
EB	674.91	13189.08	12910.85	278.23
ST	433.98	27545.44	384.66	27160.77
H2O	38.64	0	0	0
TO	1285.51	349.2	349.2	
MT	0	0	0	0
ET	0	0	0	0
BZ	276.67	0.04	0.04	0
H2	0	0	0	0

The comprehensive list of all equipments utilized in the process is shown in Table 2.4

Table 2.4. List of equipment used in the process.

Code	**Equipment type**	**Function and Comments**
Production of Hydrocarbons		
P-101	Pump	Drives the ethylbenzene from the feed tank
M-101	Mixer	Mixes the feed ethylbenzene with the recycled ethylbenzene
E-101	Heater	Preheats the ethylbenzene mixture to 157 °C from 25 °C
HEX-101	Heat exchanger	Heats the ethylbenzene mixture to 478 °C prior to entering the second mixer

P-102	Pump	Drives the water feed from the storage tank
E-102	Heater	Preheats the water feed to 760 °C before entering the second mixer
M-102	Mixer	Mixes ethylbenzene feed with the water
V-101	Valve	Reduces the pressure from 1 bar to 0.7 bar to satisfy the reactor conditions
R-101	Plug-flow reactor	Produces the first portion of the hydrocarbons
E-103	Heater	Heats the outlet from the first reactor back to 630 °C to satisfy the reactor conditions
R-102	Plug-flow reactor	Produces the final portion of the hydrocarbons
Three-phase Separation		
CR-101	Compressor	Increases the final reactor outlet to 1 bar to meet the pressure conditions for the three-phase separator
CL-101	Cooler	Cools the stream to 570 °C from 692 °C to satisfy the desired conditions of the HEX-101 heat exchanger
HEX-102	Heat exchanger	Cools the stream further to 40 °C to comply the conditions for the separation
C-101	Three-phase separator	Separates the final reactor outlet into three streams: ● hydrogen, methane, ethylene in the gas phase ● water in the liquid phase ● styrene, ethylbenzene, toluene, and benzene in the liquid phase
Styrene Purification		
DC-101	Trayed distillation column	Separates the benzene and toluene from the styrene and unreacted ethylbenzene
DC-102	Packed distillation column	Purifies the styrene stream by sending the unreacted ethylbenzene to recycling
P-103	Pump	Returns the conditions of the

		stream to initial 1 bar and drives the ethylbenzene for recycle
P-104	Pump	Directs the purified styrene to the storage tank

Chapter 3: Major equipment design

This chapter presents the design of six essential process units: one heat exchanger, two reactors, three-phase separator, and two separation units. Both theoretical and computational approaches were utilized, including detailed hand calculations and Aspen simulation analyses. The design methodology for each unit is thoroughly explained, along with the underlying working principles, ensuring a comprehensive understanding of their operation and performance.

3.1. HEX-101 heat exchanger design

Heat exchanger (HEX) is a system that transfers internal thermal energy between two or more fluids at different temperatures [34]. According to the type of heat exchanger used, gas to gas, liquid to gas, or liquid to liquid processes can occur, where fluids are divided by a heat transfer surface preventing them from direct contact [35]. Heat exchangers are used in various sectors including transportation, electricity, petroleum, refrigeration, air conditioning, heat recovery, alternative fuels, etcetera [36]. Used in both heating and cooling systems, depending on their design characteristics, such as material, components, flow configurations, there are different heat exchangers available [37].

In industry, generally 4 types of heat exchangers are used: shell and tube heat exchangers, double pipe heat exchangers, plate heat exchangers, and finned tube heat exchangers [37]. Several factors, including operating costs, fouling, corrosion propensity, pressure drop, temperature ranges, and safety concerns, influence the selection of an appropriate heat exchanger.

Shell and tube heat exchangers are used in the current styrene manufacturing process. They consist of a shell housing smaller tubes, through which hot gases from a series of reactors pass. These hot gases heat the cold stream of raw ethylbenzene flowing through the shell side [38]. As a result, both streams reach the temperatures necessary for the reaction to proceed in a gaseous state.

3.1.1. HEX-101 design calculations

The calculation of heat duty, temperature changes and pressure drops are the main objectives in the design of a heat exchanger. The initial design of the heat exchanger was started with manual calculations, which made it easy to calibrate all the parameters before starting the Aspen simulation. Since styrene manufacturing occurs under high temperatures, large surface areas of heat exchangers are required. Thus it was decided to place 4 parallel heat exchangers instead of a single one, and inlet flow rates were divided by four respectively. The process was carried out in chronological order since many parameters were prerequisites of each other. All the necessary information is presented in Table 3.1.1.

Table 3.1.1. Input Parameters for hand calculations of HEX-101.

Parameter	**Hot side**	**Cold side**
Chemical Composition	EB, ST, TO, BZ, MT, ET, H2O, H2	EB, ST, TO, BZ
Location in heat exchanger	Tube side	Shell side
Inlet temperature, ℃	570	157
Outlet temperature, ℃	445	460
Mass flow rate, kg/h	26253.70	11390.43
Inlet pressure, bar	1	1

In any exchanger overall heat transfer is governed by the following Equation (3.1):

$$Q = UA\Delta T_{LM} \tag{3.1}$$

with Q - being the overall heat transfer, U - the overall heat transfer coefficient, A - the heat transfer area, and ΔT_{LM} is the log-mean temperature difference (LMTD). LMTD was determined by the Equation (3.2) for counter-current flow, where updated inlet and outlet temperatures from PFD were used.

$$\Delta T_{LM} = \frac{(H_{in} - C_{out})(H_{out} - C_{in})}{ln(\frac{H_{in} - C_{out}}{H_{out} - C_{in}})} \tag{3.2}$$

where H_{in} - is a hot fluid inlet temperature, H_{out}- is a hot fluid outlet temperature, C_{out}- is a cold fluid outlet temperature, and C_{in}- is the inlet temperature of a cold fluid.

It was decided to keep a one-pass heat exchanger as it provides sufficient heat exchange in this system, while maintaining flow consistency and ease of access for cleaning. Because of

this configuration, a correction factor was multiplied to the LMTD to determine the true temperature difference $\Delta T_{LM\,(true)}$. Required correction factor , F_t, was obtained using the R and S ratios, as shown in Equations (3.3 - 3.5).

$$F_t = \frac{\sqrt{R^2+1}*ln(\frac{1-S}{1-RS})}{(R-1)*ln(\frac{2-S(R+1-\sqrt{R^2+1}}{2-S(R+1+\sqrt{R^2+1})})} \tag{3.3}$$

$$R = \frac{H_{in}-C_{in}}{C_{out}-C_{in}} \tag{3.4}$$

$$S = \frac{C_{out}-C_{in}}{H_{in}-C_{in}} \tag{3.5}$$

Further, to determine the heat transfer area, Q was firstly estimated by the Equation (3.6):

$$Q = c_p m\Delta T \tag{3.6}$$

where, c_p is a specific heat retrieved from Aspen, m is mass flow rate, and ΔT is a temperature difference. These values were then inserted into Equation 1, using an assumed overall heat transfer coefficient ($U_{assumed}$) to find heat transfer area $A_{assumed}$. The assumption for $U_{assumed}$ was made based on an appropriate graph from a reference data for heat transfer between two low-pressure gases. The Equation (3.7) is presented below:

$$A_{assumed} = \frac{Q}{U_{assumed}*\Delta T_{LM\,(true)}} \tag{3.7}$$

Then, the geometry of the exchanger was necessary to proceed with calculations. Exchangers' components sizing, such as inlet, outlet diameters and length, were taken from reference standard dimensions [39]. These values are listed in Table 3.1.2. Through these values, the area of tubes (A_t) and their quantity (N_t) were found by Equations (3.8-3.9).

Table 3.1.2. Geometric Parameters of Heat Exchanger Tubes.

Parameter	**Inner Diameter (D_i)**	**Outer diameter (D_o)**	**Thickness**	**Length**
Value, m	0.0286	0.032	0.0017	2.44

$$A_t = LD_o\pi \tag{3.8}$$

$$N_t = \frac{A}{A_t} \tag{3.9}$$

The next key step was to determine the bundle (D_b) and shell (D_s) diameters. A triangular pitch arrangement at 30 degrees was selected for its superior heat transfer characteristics while maintaining acceptably low pressure drops in our specific application. This configuration provides greater tube density and promotes beneficial shell-side turbulence without compromising system efficiency [39]. Since a one-pass heat exchanger configuration was chosen with this triangular arrangement, the following Equation (3.10) was used for calculation of D_b:

$$D_b = D_o\left(\frac{N_t}{K}\right)^{\frac{1}{n1}} \tag{3.10}$$

where, D_o is the outer tube diameter, N_t is the total number of tubes, and K = 0.319 and n_1= 2.142. The shell diameter was then calculated by adding the bundle clearance to the received D_b.

Using the obtained values, Reynolds and Prandtl numbers were calculated. While heat transfer factor j_h was located from the appropriate graph in the reference data [40]. These values were then used to determine the heat transfer coefficients using Equations (3.11-3.12).

$$h_t = \frac{k_f}{D_i} j_h Re^{0.33} \tag{3.11}$$

$$h_s = \frac{k_f}{D_i} j_h Re^{0.33} \tag{3.12}$$

with h_t denoting the tube-side heat transfer coefficient, k_f representing the thermal conductivity of the fluid, D_i indicating the inner diameter of the tube, and j_h representing the heat transfer factor. Similarly, the shell-side heat transfer coefficient (h_s) was computed using the equivalent parameters from the shell side.

Finally, the overall heat transfer coefficient was found using the Equation (3.13):

$$\frac{1}{U_0} = \frac{1}{h_s} + \frac{1}{h_{od}} + \frac{d_0 ln(\frac{D_0}{D_i})}{2k_{wall}} + \frac{d_0}{d_i} * \frac{1}{h_{id}} + \frac{D_o}{D_i} * \frac{1}{h_i} \tag{3.13}$$

where, U_0 is the overall coefficient based on the outside area of the tube, h_s represents outside fluid film coefficient, h_i- inside fluid coefficient, h_{od}- outside dirt coefficient, h_{id} - inside dirt coefficient, k_{wall}- thermal conductivity of the tube wall, D_o- outside diameter of the tube and D_i - inside diameter of the tube.

All calculations were done following the principles, tables and graphs from the reference data [40]. The detailed computations displayed in the Excel document titled "HEX-101 design."

3.1.2. HEX-101 specification sheet

Following the preliminary hand calculations, a detailed heat exchanger design was developed using Aspen Plus V14. The software allowed for a more precise evaluation of thermal and hydraulic performance, considering factors such as pressure drops, heat transfer coefficients, and overall exchanger effectiveness. The final design was optimized based on the process requirements, ensuring efficient heat exchange while maintaining operational feasibility.

Table 3.1.3. presents the key results obtained from the Aspen Plus simulation. These values serve as the basis for confirming the feasibility of the heat exchanger design and validating the accuracy of the hand calculations. The temperature profiles of the hot and cold fluids as a function of duty and EDR Browser data for HEX-101 are displayed in Appendix C1.

Table 3.1.3. Specification sheet for HEX-101.

Graphical representation of the equipment		
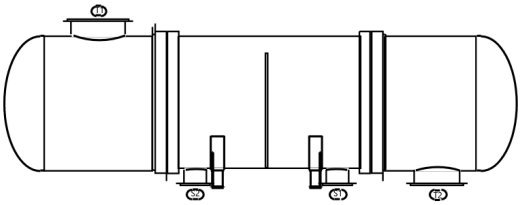	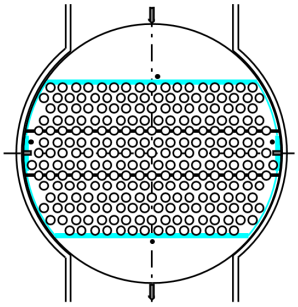	
Lengths, mm	2440	
Type	**Tube Side**	**Shell Side**
Inner diameter, mm	28.6	1692
Outside diameter, mm	32	1700
Tube pattern	30 Triangular	
Number of tube passes	1	
Number of tubes	1415	
Pitch diameter, mm	40	
Baffle spacing	0.67	
Shell in series	1	
Shell in parallel	1	
Pressure drop, bar	0.015	0.032
Material	Stainless Steel 316	

Based on reference data evaluating fabrication properties, mechanical strength, resistance to galvanic corrosion, and material cost, SS316 (316 Stainless Steel) was selected for HEX-101 design. This material offers outstanding corrosion resistance and maintains strength at elevated temperatures up to 870°C [41]. While its cost is slightly higher than other stainless steel alternatives, its durability and long-term performance make it the most suitable choice for this application [41]. Moreover, Inconel or Monel materials might be better for highly aggressive or extreme temperature environments, SS316 is the most practical and economical choice for styrene production [34].

Comparing hand calculations with Aspen results shows slight differences due to several factors. Aspen uses its built-in database for fluid properties and follows its design algorithms, while hand calculations rely on simplified assumptions. As a result, hand calculations provide an alternative design approach rather than an exact match to Aspen's output.

3.2. R-101 and R-102 Reactors design

Styrene production occurs in a gas-phase fixed-bed plug flow reactor (PFR), with the main reactor output consisting of styrene (ST), ethylbenzene (EB), water, hydrogen, benzene, toluene, ethylene, and methane. It was decided to place two PFR reactors in series, with a heater between them to maintain a stable temperature and maximize styrene conversion and yield.

This chapter details the design of Reactors R-101 and R-102, covering their dimensions, operating conditions, and materials of construction. Additionally, a key aspect of the design includes the catalyst weight and shape, which play a crucial role in optimizing reactor performance.

3.2.1. Reactor type

For manufacturing of styrene, a fixed-bed reactor was chosen due to its operational stability, efficient heat management, and suitability for catalytic reactions. Fixed-bed reactors provide uniform catalyst distribution, ensuring consistent contact between reactants and catalyst, which enhances conversion efficiency. Additionally, they offer ease of catalyst replacement and lower maintenance requirements compared to fluidized-bed reactors [42]. The structured catalyst bed also minimizes pressure drop, making it a cost-effective and scalable option for industrial styrene production. A fixed-bed reactor was chosen for styrene production due to its ability to maintain stable catalyst performance while providing high selectivity toward styrene. In contrast, fluidized-bed reactors, despite their excellent heat transfer, pose operational challenges due to catalyst attrition and handling issues. Moving-bed reactors offer continuous catalyst regeneration but involve a more complex design and higher costs. Tubular reactors without a catalyst bed would require extremely high temperatures, making them inefficient for selective styrene production.

3.2.2. General Principles of Reactor Design

In the styrene production process, a mixture of ethylbenzene and steam is thoroughly mixed and preheated to 630°C at a pressure of 0.7 bar before entering the reactor. The primary reactions involved in the process are summarized in Table 3.2.1.

Table 3.2.1. Reaction involved in styrene production.

Reaction		Type	Operating unit
R1	$C_6H_5CH_2CH_3 \rightleftharpoons C_6H_5CH = CH_2 + H_2$	main	PFR
R2	$C_6H_5CH_2CH_3 \rightarrow C_6H_6 + C_2H_4$	side	PFR
R3	$C_6H_5CH_2CH_3 + H_2 \rightarrow C_6H_5CH_5 + CH_4$	side	PFR
R4	$C_6H_5CH = CH_2 + 2H_2 \rightarrow C_6H_5CH_5 + CH_4$	side	PFR

The reaction occurs in the gas phase within a fixed-bed reactor, where the catalyst is packed in a structured bed to ensure uniform flow distribution and effective contact between reactants and catalyst surfaces. The reactor's void fraction is 0.4312, optimizing the balance between pressure drop and reaction kinetics. The reactor system consists of two multi-tube reactors arranged in series, with an intermediate heater placed between them. This heater reheats the effluent from the first reactor back to 630°C before it enters the second reactor. The entire outflow from the first reactor is directed into the second reactor without separation to maximize conversion and selectivity.

3.2.3. R-101 design calculations

The mass and molar flow rates entering the first reactor were determined based on the reaction stoichiometry and the desired conversion. The molecular weight of the feed was used to convert between mass and molar flow rates using the Equation (3.14):

$$\overline{n} = \frac{\overline{m}}{M} \tag{3.14}$$

where, $\overline{n}$ denotes molar flow rate , $\overline{m}$ - mass flow rate, M - mixtures molar mass.

The molar density of the feed was obtained from Aspen, using the specified operating temperature and pressure conditions. Using this molar density, the volumetric flow rate was determined as follows (Equation 3.15):

$$\overline{Q} = \frac{\overline{n}}{\rho} \tag{3.15}$$

where, $\overline{Q}$ - volumetric flow rate, $\overline{n}$ - molar flow rate, ρ - density of the fluid.

The volumetric flow rate into the reactor was utilized to determine the required superficial velocity, which was then used to size the diameter and volume of the plug flow reactor (PFR).

The catalyst loading was calculated based on the desired conversion and reaction kinetics. The total catalyst volume was obtained using the catalyst weight and density, as shown by Equation 3.16:

$$V_{cat} = \frac{W_{cat}}{\rho_{cat}} \tag{3.16}$$

where, V_{cat} - volume of the catalyst, W_{cat} - weight of the catalyst, ρ_{cat} - density of the catalyst

To determine the total reactor volume, the catalyst volume was adjusted for voidage and a 20% safety margin (Equation 3.17). The 20% safety factor is applied to the reactor volume to account for uncertainties in design, operational variability, and potential future adjustments. Over time, catalyst particles may settle, reducing the effective reactor volume, and variations in packing density can affect the void fraction. Changes in operating conditions such as temperature, pressure, or flow rates may also impact reaction kinetics, requiring additional space for adjustments. The extra volume ensures stable flow conditions, prevents excessive pressure drops, and provides flexibility for future process modifications. Since real-world conditions often differ from theoretical calculations, this margin helps maintain reliable reactor performance:

$$V_{PFR} = \frac{V_{cat}}{1-\varepsilon} \times 1.2 \tag{3.17}$$

where V_{PFR} - volume PFR, V_{cat} - volume of catalyst, ε-void fraction

The reactor dimensions, including diameter and length, were chosen to accommodate the required volume while maintaining an optimal superficial velocity to ensure efficient flow and minimize pressure drop. To achieve a velocity within the desired range of 3–5 m/s, the reactor

was designed with eight parallel tubes, each with a diameter of 1.85 m. A superficial velocity of 3–5 m/s ensures efficient mass transfer and turbulent flow, which enhances reactant mixing and catalyst contact in the PFR. This velocity range prevents excessive pressure drop while avoiding poor mass transfer that can occur at lower velocities. It also helps maintain uniform flow distribution, optimizing catalyst utilization and reaction efficiency. The superficial velocity was then determined using the volumetric flow rate and the total cross-sectional area (Equation 3.18).

$$u_s = \frac{\overline{Q}}{A} \tag{3.18}$$

where u_s- superficial velocity of the fluid, $\overline{Q}$ - volumetric flow rate of the fluid. A - cross-sectional area of a single tube.

Finally, the reactor length was calculated based on the required volume, the selected tube diameter, and the number of tubes to ensure proper reactor sizing (Equation 3.19).

$$\mathrm{L} = \frac{4V_{PFR}}{N_{tubes} \times \pi \times D_{in}^{\ 2}} \tag{3.19}$$

where L - length of the tube, N_{tubes}- number of tubes, D_{in}- internal diameter of the reactor.

The pressure drop across the reactor was estimated using the Ergun equation (3.20), which accounts for fluid density, viscosity, and catalyst particle size:

$$\frac{\Delta P}{L} = \frac{150\mu(1-\varepsilon)}{d_p^{\ 2}\varepsilon^3\theta^2} \times \frac{q}{A} + \frac{1.75\rho(1-\varepsilon)}{d_p\,\varepsilon^3\theta} \times \left(\frac{q}{A}\right)^2 \tag{3.20}$$

where ΔP denotes for the pressure drop, L - the length of the porous bed, μ - fluid viscosity, ε- the porosity of the fluid, d_p - the average particle diameter, θ - shape factor, q - volumetric flow rate, A- cross sectional area, ρ - the fluid density

The reactor material was selected based on its ability to withstand high temperatures and corrosive conditions. SS316L stainless steel was chosen due to its high-temperature resistance, corrosion resistance, and mechanical strength.

The required wall thickness was determined using ASME B31.3, considering the operating pressure, allowable stress, and corrosion allowance (Equations 3.21-3.22).

$$t_m = t_p + c \tag{3.21}$$

$$t_p = \frac{Pd}{2(SE + P\gamma)} \tag{3.22}$$

where t_m - minimum required thickness, t_p - pressure design thickness, c - sum of mechanical allowances, P- internal design gauge pressure, d - pipe outside diameter, S- basic allowable stress for pipe material, E- casting quality factor, γ - temperature coefficient

All the important calculations are presented in the ESI Excel file called “R-101, R-102”.

3.2.4. R-101 unit specification sheet

The unit specification sheet in Table 3.2.1. was developed using Aspen simulation results. During calculation of the reactor volume, the inner diameter only was considered, since it was specified in the reactor parameters in Aspen simulation. Corrosion resistivity, mechanical strength, thermal stability make stainless steel an optimal material for the reactor design.

Table 3.2.1. Specification sheet for R-101.

	R-101	**R-102**
Schematic	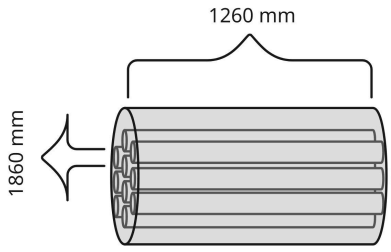	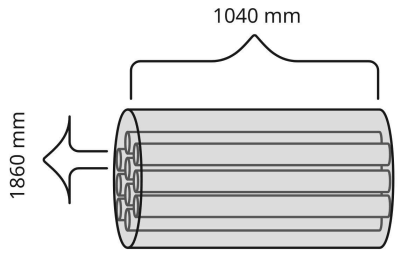
Temperature, °C	626	630
Outlet Temperature, °C	546	582
Pressure, bar	0.693	0.592
Inlet pressure, bar	0.700	0.686
Pressure drop, bar	0.0145	0.187
Number of Tubes	10	10
Inside diameter of single tube, mm	1850	1850
Wall thickness required, mm	5	5
Outside diameter of single tube, mm	1860	1860
Length, mm	1260	1040
Material Selection	**SS316L [43]**	

Allowable Stress, MPa	124.106	
Corrosion allowance, mm	3	
Weld strength reduction factor	1	
Coefficient of material used	0.4	
Weld quality factor	1	
Catalyst Data	Fe2O3	
Weight, kg	40000	33068
Bed voidage	0.4312	
Diameter of particle, mm	5.5	
Height, mm	5.5	
Shape	Cylindrical	
Shape factor	0.874	

3.3. C-101 Three-Phase Separator Design.

After moving out of the PFR system, the hot effluent is cooled before being directed to the three phase separator, C-101. The mixture is then separated into three phases, leaving significant amounts of water and gas (hydrogen, methane, and ethane) eliminated. This section will cover the design and operational principles of the C-101 three phase separator used in this process.

2.3.1 The working principle of the three phase separator.

Three-phase separator is an important unit operation in chemical engineering for separating vapor, organic liquid, and aqueous liquid phase. This technique works on the principle of volatility, density, and immiscibility differences between components to achieve successful separation. In our case, the components to isolate are non-condensable gases (H2, CH4), organic liquids(styrene, ethylbenzene), and water in liquid phase.

The feed stream exiting the reactor at a high temperature of 600°C and 1.044 bar is cooled to 40-60 °C before entering the separator. Because of the pressure drop and significant difference in boiling points, and mutual immiscibility, the three separate phases form. Hydrogen, Ethylene, and Methane, which have low boiling points of -253°C, -104°C, -162°C respectively, evaporate very quickly, while the rest of the components remain liquid with high efficiency. The

operating condition of temperature 40°C and pressure 1 bar was carefully chosen to ensure maximum gas recovery, efficient condensation of organics, and high phase purity.

3.3.2 Multicomponent separator analysis.

The design of three phase separators is based on a detailed analysis of thermodynamic framework, phase equilibrium behavior, and stream compositions. The separation process is based on three key principles, which are Vapor-Liquid Equilibrium (VLE), Liquid-Liquid Equilibrium (LLE), and Henry's Law. The volatile components, such as H2 and CH4, remain in the gas phase due to their high volatility, while organic components, such as styrene and ethylbenzene, condense into the liquid phase due to low volatility. Also, this can be justified by vapor pressure data and K-value calculations. Using modified Raoult's Law (Equation 3.23),

$$K_i = \gamma_i \frac{P_i^{sat}}{P} \tag{3.23}$$

where, K_i is VLE ratio, γ_i is activity coefficient, P_i^{sat} is pressure, and P is operating separator pressure, we can confirm the efficient separation of gas and liquid phases based on volatility of components.

The LLE behavior of water and organics, namely water-styrene and water-ethylbenzene, systems was analyzed using mutual solubility data from NIST WebBook. The experimental LLE data from NIST in Aspen Plus for the water-styrene and ethylbenzene-styrene system in Table 3.3.2 below confirm that water and hydrocarbons are nearly immiscible.

Table 3.3.2. Experimental LLE data from NIST for the water-styrene and water-ethylbenzene systems.

System	Temperature(°C)	Pressure(bar)	Mole Fraction(Water in Organic)	Mole Fraction(Organic in Water)
Water-Styrene	60	1.01	0.0069	7.8038*10^-5
Water-EB	56.74	1.01	0.007467	3.9900*10^-5

The extremely low solubility of styrene and EB in water ensures that more than 99.99% of water remains in aqueous phase, while low solubility of water in the organic phase ensures

high purity of organic stream. This behavior is set by the polarity difference between water and organics, causing the separation of two liquid layers, which confirms the applicability of the three-phase separator.

Lastly, using Henry's Law for solubility of gases (Equation 3.24),

$$C = k_H(T) \bullet y_i \bullet P \tag{3.24}$$

where, C is Gas concentration in liquid (mol/kg), $k_H(T)$ is Temperature-dependent Henry's constant (mol/(kg·bar)), y_i is mole fraction of i in the vapor phase, and P system pressure, we confirm that non-condensable gases have negligible solubility in the aqueous and organic phases at 60°C and 1.2 bar. Since there is no available data for Henry's constant at 60°C and 1.2 bar, we can estimate it using the Equation (3.25) [44]:

$$k_H(T) = k_H^{\circ} \bullet exp\left(\frac{d(lnk_H)}{d(1/T)}\left(\frac{1}{T} - \frac{1}{298.15}\right)\right) \tag{3.25}$$

where, k_H° at Henry's constant at 25°C, and $\frac{d(lnk_H)}{d(1/T)}$ temperature sensitivity.

Table 3.3.3. Henry's Constants at 60°C

Gas	k_H° **(mol/(kg·bar))**	$\frac{d(lnk_H)}{d(1/T)}$**(K)**	$k_H(T)$**(mol/(kg·bar))**
H2 [44]	0.00078	500	0.000654
C2H4 [45]	0.0047	1800	0.00249

Using values of temperature sensitivity 500K for hydrogen, and 1800K for ethylene, we calculate Henry's constants at 60°C and 1.2 bar. Also, the concentration was converted to mole fraction using molarity of water 55.5 mol/kg.

Table 3.3.4. Solubility of gases in Water

Gas	**Concentration(mol/kg)**	**Mole fraction(x_i)**
H2 [44]	0.0000785	1.41*10^-6
C2H4 [45]	0.0000346	6.24*10^-7

As we can see, Henry's Law confirms that hydrogen and ethylene solubility in water at 60°C and 1.2 bar is negligible (< 0.0002%). This justifies simplifying the process model by assuming all gas exits in the vapor phase. Moreover, the system effectively partitions the feed into an organic liquid phase containing styrene and ethylbenzene, and an aqueous liquid phase containing water. The chosen operating conditions (40°C and 1 bar) ensure efficient separation while keeping high purity requirements.

3.4. DC-101 Distillation Column

The distillation column DC-101 is used to separate ethylbenzene and styrene from benzene, toluene, and what is left from three-phase separation. The feed conditions remained unchanged and read as 40°C and 1 bar. However, the operating conditions of the column are lower in regards to pressure, as they advocate for optimal temperature of the bottom stream, which is fed to the next distillation column.

3.4.1. DC-101 Distillation Column Working Principle

The main working principle of the distillation is based on the relative volatility of components with respect to the heavy key component. The distillate consists of the components which have higher relative volatilities, while non-volatile components descend to the bottom stream.

As vapor rises up from the bottom, it steps into the contact with the liquid that falls from the top of the column. With any time contact takes place, there is a dynamic equilibrium between the two, and the contact area serves as a medium for mass transfer between the two phases. The trays inside the column are designed to enhance this contact. Furthermore, the reflux ratio also plays an important role in the quality of separation, since it affects the equilibrium conditions.

To effectively separate EB and ST from other components, it is necessary to create an optimum design. It consists of a careful combination of reflux ratio, tray spacing, column diameter, and the number of stages. In addition, because the relative volatility is not constant due to the temperature difference in the column, it was decided to take a geometric mean of relative volatilities at condenser and reboiler conditions.

3.4.2. Relative Volatility of the Components

The relative volatility was calculated through the ratio of saturation pressures of components (Equation 3.26).

$$\alpha_{i,j} = \frac{P_{sat,i}}{P_{sat,j}} \quad (3.2$$

where, $P_{sat,i}$ and $P_{sat,j}$ are the saturation pressures (mm Hg) of components i and j, and $\alpha_{i,j}$ is the relative volatility of the component i with respect to j.

The saturation pressure of these components, in turn, is found from the Antoine Equation [46]:

$$log\, P_{sat} = A - \frac{B}{T + C} \quad (3.2$$

where, A, B, and C are the Antoine coefficients, which can be retrieved from the table X, and T is the temperature (K).

The concentrations of MT, ET, H2 are so low, so it was concluded to neglect them from calculations, and the rest are displayed in the table below.

Table 3.4.2. Saturation pressures and relative volatilities of the entering components.

Components	Condenser		Reboiler		Mean Volatility
	P_{sat}, mm Hg	Relative Vol.	P_{sat}, mm Hg	Relative Vol.	
EB [47]	0.033	1	0.033	1	1
ST [48]	0.023	0.70	0.022	0.67	0.69
TO [49]	0.27	8.14	0.27	8.14	8.14
BZ [50]	0.09	2.71	0.09	2.71	2.71
H2O [51]	0.086	2.60	0.013	0.39	1.00

According to the boiling temperatures of the components, TO was chosen to be the light key component, and EB to be the heavy key (reference component). The relative volatilities of BZ and TO are higher than of other components, which means that their separation from the heavy component will happen. The desired top stream product would consist of the liquid mixture of water, BZ, and TO. The bottom product is a mixture that mainly consists of ST and EB with negligible fractions of other components.

3.4.3. DC-101 Column Design

The number of theoretical and actual stages with reflux ratios is calculated using the Frenske-Underwood-Gilliand (FUG) method [52].

The equation for calculating the number of theoretical stages looks as follow (Equation 3.28):

$$N_{min} = \frac{log\left[\left(\frac{x_{LK}}{x_{HK}}\right)_d \left(\frac{x_{HK}}{x_{LK}}\right)_b\right]}{log(a_{LK})} \tag{3.28}$$

where, a_{LK} is the relative volatility of the light key component, x_{LK} and x_{HK} are the molar fractions of the light key and heavy key component respectively, with d and b referring to the bottom and distillate streams of the column, resulting in the N_{min} value of 5.59.

The reflux ratio, in turn, is derived from the Underwood correlation [52]:

$$\sum \frac{\alpha_i x_{i,d}}{\alpha_i - \theta} = R_{min} + 1 \tag{3.29}$$

where, α_i is the relative volatility of the respectful component, $x_{i,d}$ is the molar fraction of the component in the distillate stream, R_{min} is the minimum reflux ratio, and θ is the root of the equation.

To find θ, which should be in a range between the relative volatilities of the heavy and light key components, is found numerically from the following expression [52]:

$$\sum \frac{\alpha_i x_{i,f}}{\alpha_i - \theta} = 1 - q \tag{3.30}$$

where, α_i is the relative volatility of the respectful component, $x_{i,f}$ is the molar fraction of the component in the feed stream, and q is the quality of the feed stream.

As the feed stream at 40 °C and 1 bar is in the form of a saturated liquid, the quality of the feed was taken as 1. The subsequent calculations yielded the value of θ to be ~2.43, giving a minimum reflux ratio to be 1.967. The actual reflux ratio, which is normally in the range between 1.2 to 1.5 the value of minimum reflux ratio, was decided to be taken as $1.5R_{min}$ to provide the maximum separation efficiency.

The Gilland correlation [52] is used to determine the actual number of theoretical stages at a given reflux ratio:

$$\frac{N-Nmin}{N+1} = 1 - exp\left(\frac{1+54.4\psi}{11+117.2\psi} * \frac{\psi^{-1}}{\psi^{0.5}}\right) \quad (3.31)$$

where, N_{min} is the minimum number of stages, N is the actual number of stages, and ψ is the correlation coefficient, which is calculated from the following Equation (3.32) [52]:

$$\psi = \frac{R - Rmin}{R+1} \quad (3.32)$$

where, R and R_{min} are the actual and minimum reflux ratios.

After calculation, the correlation coefficient was equal to ~0.25, which gives the N value of 10.36.

Values for R_{min}, R, N_{min}, and N can be found in the Table (3.4.3).

Table 3.4.3. Minimum and actual values of reflux ratio and number of stages.

R_{min}	**R**	**N_{min}**	**N**
1.967	2.95	5.59	10.36

The feed stage for the column was chosen based on the DSTWU unit in the Aspen V14.0, which identified that the optimal feed should be located on stage 8. In addition, the actual number of theoretical stages was increased to 25 to obtain the purity of the bottom stream to be 99% mixture of EB and ST. The reflux ratio was also increased to 4 to further increase the separation.

3.4.4. DC-101 Distillation Column Specification Sheet

The specification sheet for the DC-101 column can be seen in the table below.

Table 3.4.4. Specification sheet of the DC-101 distillation column.

Unit type	DC-101	**Schematic diagram**

Specification	Distillation column	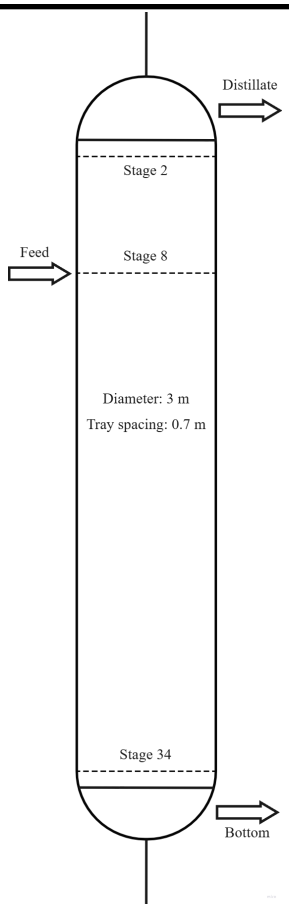	
Height, m	16.1		
Number of stages	25		
Reflux ratio	4		
Inlet conditions			
Temperature, °C	40		
Pressure, bar	1		
Condenser conditions			
Type	Total		
Temperature, °C	3.24		
Pressure, bar	0.3		
Reboiler conditions			
Type	Kettle		
Temperature, °C	110.46		
Pressure, bar	0.41		
Mass flow rate, kg/h		**Internal design**	
Feed	43793.47		
Distillate	2709.71	**Tray type**	Sieve
Bottoms	41083.76	**Tray spacing**	0.7 m
Material	SS-316L [53]	**Diameter**	3 m

The material selection for the column consists of several factors: corrosion resistance, pitting resistance, unreactivity with major components, mechanical strength, and thermal conditions suitability. Due to the presence of water in the feed stream, it is especially important to account for the material corrosion. The standard choice for such circumstances falls on the different kinds of stainless steel-based materials. The final comparison was carried out between SS-316 and SS-316L, however, it was decided to opt for SS-316L, as it contains less carbon than SS-316 [53]. This, in turn,even further prevents the possibility of sensitization, reducing the intergranular corrosion in heat-affected zones, meaning that welds will maintain their structural integrity.

3.4.5. DC-101 Design Plots

The plots for the molar composition, temperature profile, pressure profile, and molar flow rates can be found in Appendix E.

In Figure E1, it can be seen that there is a steady pressure increase in the column from 0.3 bar at the 1st stage (condenser) up to 0.41 bar at the 25th stage (reboiler).

Figure E2 represents the molar flow rate inside the column. The spike increase in the molar flow rate of the liquid at the 8th stage (feed stage) is due to the fact that the feed to the column is in the liquid phase.

Figure E3 shows that the temperature rises from stage 1 to stage 25 due to the presence of condensation and reboiling at the respectful stages. The liquid coming down the column is heated, as it turns to vapor, and vapor that is reboiled turns into liquid at the condenser, thereby decreasing the temperature.

From Figure E4, it is evident that the liquid molar fraction of EB experienced a sharp decrease at the feed stage due to the high difference in flow rates between the distillate and bottom streams.

3.5. DC-102 Vacuum distillation column

DC-102 unit separates styrene and ethylbenzene in the feed stream, collecting 99% of styrene in bottoms as final product, and recycling 98% of ethylbenzene back to the system. Feed conditions are that of the bottom stream of DC-101 unit, temperature is 11℃ and pressure is 0.41 bar. The feed temperature is close to the bubble point of the stream, T_{bub}=110.62℃, so it is considered a saturated liquid. The recovery of components in the distillate other than styrene and ethylbenzene are considered as 1, so they are neglected in the design calculation. The operating conditions are taken from Report 2, and presented in Table 3.5.3.

3.5.1. Stage number and reflux ratio

Firstly, the saturation pressures and relative volatilities of each component were calculated by Eq (3.27) and Eq (3.26), respectively, at the condenser and reboiler temperatures,

and presented in Table 3.5.1. For further calculations, the geometric means of relative volatilities at two temperatures were taken.

Table 3.5.1. The calculated relative volatilities of each component.

	Condenser, T=77°C		**Reboiler, T=113°C**		**Geom. mean**
	Psat, mmHg	**α**	**Psat, mmHg**	**α**	**α**
EB	112.0604	1.3900	390.0036	1.3134	1.3512
ST	80.6162	1	296.9473	1	1

Calculated minimum stage number by Eq (3.28) is 30.54 and calculated minimum reflux ratio by Eq (3.29) is 7.963. However, these values do not align with values obtained in Aspen as discussed in Appendix F. Minimum stage number from Aspen is 37.1 and minimum reflux ratio is 11.7. After several tries to increase product styrene purity and sensitivity analysis in Aspen, the number of stages is taken 80 and reflux ratio is 16.34, more explanations are given in Appendix F.

3.5.2. Packing type selection and column sizing

MellapakPlus 252Y was selected as the best packing material in terms of higher product purity and the styrene monomer capacity according to Salem and Shokrkar [54]. The main characteristics of the selected packing type, that are used in column internals calculations, are presented in Table 3.5.2.

Table 3.5.2. Characteristics of the packing [19].

Packing	**Type**	**Material**	**Size**	F_p, **ft²/ft³**	**a, m²/m³**	**ϵ, m²/m³**
MellapakPlus	Structured	Metal	252Y	12	250	0.98

The inner diameter of the column is calculated by Eq (3.33) [52]:

$$D_i = \left(\frac{4VM_V}{f u_V \pi \rho_V}\right)^{0.5} \tag{3.33}$$

where, D_i is the column inner diameter in m, V is vapor molar flow rate in kmol/h, M_V is vapor molar mass in kg/kmol, ρ_V is vapor mass density in kg/m³, u_V is the superficial vapor velocity in m/s, f is the fraction of flooding. f should be between 50 and 70% [52], and in this report it is taken as 70%. The calculated inner diameter is 6.55 m with more extensive calculation given in

Appendix F. However, the diameter of 5.9 m was chosen in column design according to the hydraulic plots in Aspen; more detailed explanations are given in Appendix F.

The shortcut method for HETP calculation, Eq (3.34) [55], is applied for vacuum distillation of organic systems in structured packed columns. The calculated HETP is 0.526 m, it was rounded to 0.5 m for further use in the Column internals section of the Radfrac unit in Aspen.

$$HETP = \frac{5.4\sqrt{\rho_L}}{a\left(1+0.78\left(\frac{\rho_V}{\rho_L}\right)^{0.25}\cdot 10^{5.8\cdot 10^{-4}a}\right)} \tag{3.34}$$

where, ρ_L and ρ_V are liquid and vapor mass density in kg/m³, a is the specific surface area of the packing in m^{-1} from Table 3.5.2.

The minimum wall thickness and the minimum ellipsoidal head thickness are calculated by Eq (3.35) and Eq (3.36) that are specified by ASME BPV Code [56].

$$t_{wall} = \frac{PD_i}{2SE - 1.2P} \tag{3.35}$$

$$t_{head} = \frac{PD_i}{2SE - 0.2P} \tag{3.36}$$

where, t_{wall} is the wall thickness in mm, t_{head} is the head thickness in mm, P is the design pressure in N/mm², S is the maximum allowable stress in N/mm², E is the joint efficiency that is taken as 0.85 in this report [56]. The design pressure and temperature are the largest pressure and temperature in the column, that are reboiler conditions multiplied by a factor of 1.1 considering 10% for safety reasons [56]. The maximum allowable stress for material selected, Stainless steel 316L, at design temperature is 115 N/mm² according to ASME BPV Code Sec. II Part D [56].

The vessel experiences stresses due to several sources of loading, including pressure, dead weight of vessel and packing, and wind [56]. The maximum stress on the column is 92.67 N/mm², and the extensive calculations are given in Appendix F. Since the maximum stress on the column is lower than the maximum allowable stress, calculated wall and head thicknesses are valid.

3.5.3. DC-102 unit Specification sheet

The specification sheet for the DC-102 distillation column unit is shown in Table 3.5.3.

Table 3.5.3. DC-102 unit Specification Sheet.

<table>
<tr><th colspan="2">Schematic diagram</th><th colspan="2">Operating conditions</th></tr>
<tr><td colspan="2" rowspan="19"> 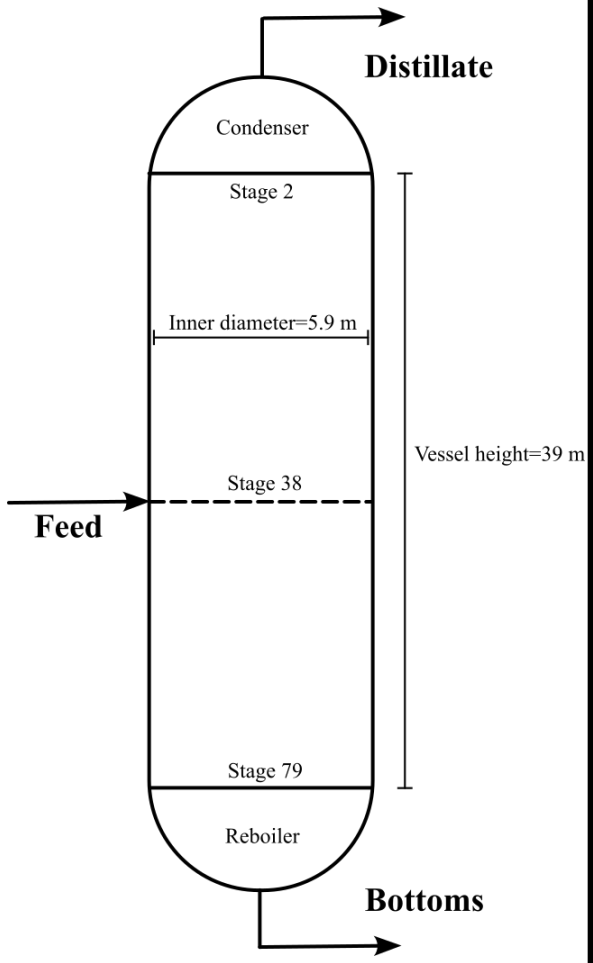
</td><td>Feed flow rate, kmol/hr</td><td>394.343</td></tr>
<tr><td>Feed temperature, °C</td><td>111</td></tr>
<tr><td>Feed pressure, bar</td><td>0.41</td></tr>
<tr><td>Distillate flow rate, kmol/hr</td><td>130.133</td></tr>
<tr><td>Bottoms flow rate, kmol/hr</td><td>264.210</td></tr>
<tr><td>Reflux ratio</td><td>11.7</td></tr>
<tr><td>Stage number</td><td>80</td></tr>
<tr><td>Feed stage</td><td>38</td></tr>
<tr><td colspan="2">Condenser conditions</td></tr>
<tr><td>Type</td><td>Total</td></tr>
<tr><td>Temperature, °C</td><td>77</td></tr>
<tr><td>Pressure, bar</td><td>0.15</td></tr>
<tr><td>Heat duty, MW</td><td>-24.84</td></tr>
<tr><td colspan="2">Reboiler conditions</td></tr>
<tr><td>Type</td><td>Kettle</td></tr>
<tr><td>Temperature, °C</td><td>113</td></tr>
<tr><td>Pressure, bar</td><td>0.40</td></tr>
<tr><td>Heat duty, MW</td><td>21.96</td></tr>
<tr><td colspan="2">Column internals</td></tr>
<tr><td>Stage interval</td><td>2-79</td></tr>
<tr><td>Inner diameter, m</td><td>5.9</td></tr>
<tr><td>Height, m</td><td>39</td></tr>
<tr><td>Wall thickness, mm</td><td>6.35</td></tr>
<tr><td>Head thickness, mm</td><td>5.55</td></tr>
<tr><td>Outer diameter, m</td><td>5.913</td></tr>
<tr><td colspan="2">Packing material specifications</td><td colspan="2">Construction material specifications</td></tr>
<tr><td>Type of packing</td><td>MellapakPlus</td><td>Construction material</td><td>Stainless steel</td></tr>
<tr><td>Material of packing</td><td>Metal</td><td>Grade</td><td>316L</td></tr>
<tr><td>Size</td><td>252Y</td><td>Stress allowed, N/mm²</td><td>115 [56]</td></tr>
<tr><td>Packing factor, ft^{-1}</td><td>12</td><td>Maximum stress, N/mm²</td><td>92.67</td></tr>
<tr><td>Specific surface area, m^{-1}</td><td>250</td><td>Corrosion allowance, mm</td><td>2 [56]</td></tr>
<tr><td>Void fraction</td><td>0.98</td><td>Joint efficiency</td><td>0.85</td></tr>
</table>

Chapter 4: Minor equipment design

In this chapter, we present the design of minor equipment, including pumps, heat exchangers, heaters, coolers, compressors, and storage tanks, all essential for the efficient operation of the styrene production process. The pump design ensures proper pressure adjustments for various process streams, with efficiency considerations factored into power calculations. Heating and cooling units are designed to regulate process fluid temperatures, ensuring optimal conditions for reaction and separation, while the compressor increases the pressure of the reactor outlet stream for seamless progression through the system. Finally, storage tanks are carefully designed to maintain the stability of raw materials and products, with specific considerations for styrene to prevent polymerization.

4.1. Pump design

In this production process, pressure-changing equipment is utilized. Since most of the process fluids exist in the liquid phase, pumps were incorporated into the Aspen Plus simulation with an assumed efficiency of 80%. The pump operations are categorized based on their function within the process. P-101 is responsible for increasing the pressure of the raw ethylbenzene stream before it enters the heating stage. P-102 is used to pressurize water in its liquid state before it undergoes heating. P-103 facilitates the recycling of ethylbenzene by pumping it out of the distillation column and directing it back to mix with the raw ethylbenzene feed. Finally, P-104 is used to pressurize the final styrene product, ensuring it reaches the required conditions for further processing or storage.

The design of these pumps requires evaluating the final power requirement, similar to the approach used for the compressor. However, a different equation is applied, as expressed in Equation (4.1):

$$W = V\Delta P \tag{4.1}$$

where W represents the power required by the pump, V is the volumetric flow rate of the fluid, and ΔP denotes the pressure difference across the pump.

To determine the actual power consumption, the calculated power value is divided by the pump efficiency, which is set at 80%. The inlet and outlet pressures, along with the corresponding power requirements for each pump, are summarized in the table 4.1.1.

Table 4.1.1. Pump Design Parameters.

Pump	Inlet Pressure, bars	Outlet Pressure, bars	Power, kW
P-101	1	1.15	0.192
P-102	1	1.15	0.312
P-103	0.15	1	0.493
P-104	0.4	1	0.609

This structured approach ensures that the pressure-changing requirements are met efficiently while optimizing power consumption in the process.

4.2. Heater, coolers and boiler design

In this process, multiple heating and cooling units are required since various liquids enter at different temperatures. To ensure the main production proceeds efficiently, it is essential to adjust the temperatures of the process fluids to the desired levels. When designing such equipment, determining the heat duty is crucial. This can be calculated using the following Equation (4.2):

$$Q=C_p \times \overline{m} \times \Delta T \tag{4.2}$$

where Q represents the heat duty of the heating or cooling unit, $\overline{m}$ is the stream's mass flow rate, C_p is the heat capacity of the substance, and ΔT is the temperature change.

4.2.1 The design values of heaters

The process involves three heaters, each serving a specific function. Heater E-101 is used to heat and vaporize ethylbenzene (EB). Heater E-102 generates steam by heating water. E-103 is used for intermediate heating between reactors. Detailed specifications of these heaters are provided in Table 4.2.1.

Table 4.2.1. The design values of heaters.

Parameter	E-101	E-102	E-103
Inlet T, degC	41.4	25	546

Outlet T, degC	157	760	630
Duty, kW	7175	65408	5962
Phase change	+	+	-

4.2.2 The design of cooling heat exchanger and cooler

Two units were employed for temperature reduction in the process: the heat exchanger HEX-102, located upstream of the three-phase separator, and the cooler CL-101, which reduces the temperature of the stream exiting the compressor. HEX-102 plays a crucial role in partially condensing the vapor-phase stream into a liquid, thereby enabling efficient downstream separation. Table 4.2.2 summarizes the duty values obtained from Aspen simulations, offering key insights into the thermal performance of both the heat exchanger and the cooler.

Table 4.2.2. The design value of cooling heat exchanger

Parameter	**HEX-102**	**CL-101**
Inlet T, degC	441	692
Outlet, degC	40	570
Duty, kW	-62477	-8805
Phase change	+	-

4.3. Compressor Design

In the process, there is a need for the pressure increase of the R-102 outlet stream pressure from 0.5 bar to 1 bar, so it can comfortably enter the subsequent heat exchanger and later separation. For such purposes, it was decided to use an isentropic compressor. Also, it is crucial to account for the duty value of the compressor that is calculated by the following Equation (4.3):

$$W = \frac{(P_2 \times V_2) - (P_1 \times V_1)}{1-\gamma} \quad (4.3)$$

where, W is the duty of the compressor, P_1 and P_2 are the pressures of the inlet stream and outlet stream, V_1 and V_2 are the inlet and outlet volumetric flow rates, and γ is the specific heat ratio of the component to be compressed. The value from the Equation 4.3 then needs to be divided by the isentropic efficiency of the pump.

The design values of the CR-101 unit can be seen in the Table (4.3.1) below.

Table 4.3.1. CR-101 design values.

Inlet pressure, bar	Outlet pressure, bar	Inlet temperature, °C	Outlet temperature, °C	Duty, kW
0.5	1	582	692	7976

4.4. Storage tanks

In the industrial production of styrene, proper design of storage tanks is important to ensure a continuous and efficient operation, and to prevent contamination, polymerization, and safety hazards. In this process, fluids such as a raw material (EB) and products (ST, BZ/TO) need to be stored before entering the process and after collection for further sale. Based on the process, three storage tanks were designed and design specifications are presented in Table 4.4.1.

The total volume needed for the storage of each component is calculated by Equation (4.4):

$$V = Q \cdot t \tag{4.4}$$

where, V is the total storage volume, Q is the volumetric flow rate of the component, t is the storage time of the component. The storage time is determined based on the safety considerations and supply chain logistics. Styrene is the most unstable component among all components to be stored, so the storage time of all components is assumed and based on the shelf life of styrene and shipping schedule.

Components other than styrene are relatively stable compared to styrene, so they can be stored at ambient temperature and atmospheric pressure, whereas styrene needs to be stored at a temperature lower than 20℃, and mixed with the inhibitor (TBC) to prevent polymerization.

Table 4.4.1. Storage tank design specifications.

Storage tank	T-101	T-102	T-103
Stored material	EB	ST	BZ/TO
State	liquid	liquid	liquid
Temperature, ℃	25	20	25
Pressure, bar	1	1	1
Flow rate, m³/year	322679	291706	27912

Storage time, months	1	1	1
Total volume, m³	26890	24309	2326
Volume of 1 tank, m³	10000 [57]	10000 [57]	3000 [58]
Number of tanks	3	3	1
Material of tanks	SS316	SS316	SS316

Chapter 5: Plant Location and Layout

Identifying a suitable site for establishing an industrial facility, along with determining its internal configuration, is critical to the success of any chemical production operation. These decisions significantly influence the efficiency and economics of the production process, the environmental footprint, and the facility's long-term adaptability. This chapter discusses the key strategic factors guiding the selection of the plant site and outlines the layout considerations implemented for the proposed styrene production facility.

5.1. Plant Site Location

The selection of an appropriate site for the styrene production plant is a crucial decision that directly impacts both the operational efficiency and economic feasibility of the project. Several key factors must be considered during site evaluation. First, access to utilities and infrastructure - including water, electricity, steam, transportation networks, and ports - is vital to support continuous operations [59]. Second, proximity to raw materials such as ethylbenzene is essential to reduce transportation costs and ensure a steady feedstock supply [59]. Third, environmental and safety regulations must be taken into account, especially due to the hazardous nature of styrene and its by-products [59]. A location that facilitates compliance with emission standards and safety codes is preferred. Additionally, closeness to major styrene-consuming markets can minimize logistics expenses and improve customer responsiveness. The availability of skilled labor is another important criterion, as the plant will require experienced engineers, operators, and maintenance personnel [59]. Lastly, geopolitical availability, referring to the site's access to international trade routes, well-developed railways, and proximity to multiple regional markets, is essential for enabling efficient product distribution and cross-border operations [59]. These factors are fundamental in determining a location that balances operational practicality with economic return [59].

5.1.1. Availability and Cost of Utilities

Pavlodar was selected as the preferred site due to its robust utility infrastructure and favorable investment environment. The region's inclusion in the Pavlodar Special Economic Zone (SEZ), established in 2011 and spanning 1,100 hectares in the Northern Industrial Zone, supports the growth of the chemical and petrochemical industries. The SEZ offers zero tax benefits, state support, and advanced infrastructure tailored to energy-intensive operations such as styrene production[60].

Pavlodar's SEZ is equipped with essential utility systems, including power, gas, water, transportation, and customs support. The presence of multiple thermal power stations, including Pavlodar CHP-3 in the Northern industrial area, ensures a stable electricity supply vital for equipment like compressors and heat exchangers[61].

In terms of water availability, Pavlodar lies within the Irtysh River Basin, which contains 34.5% of Kazakhstan's total water resources, the highest share among all eight national basins. This abundance is particularly beneficial for styrene production, where steam generation and cooling systems are water-intensive. The availability of natural water resources reduces the need for extensive recycling systems and supports continuous plant operation [62].

Utility costs in Pavlodar SEZ are competitive: electricity at 27.56 KZT/kWh, heat at 8,242.45 KZT/Gcal, and technical water at 56.76 KZT/m^3[63]. These stable tariffs improve operational predictability and enhance the plant's economic attractiveness.

Overall, the strategic location, resource abundance, and industrial infrastructure of Pavlodar present a compelling case for the establishment of a styrene production facility. Its integration into a well-supported SEZ and access to both electric and water utilities strongly align with the technical and operational demands of styrene manufacturing.

5.1.2. Proximity to Raw Materials

Styrene production primarily depends on ethylbenzene and an iron oxide catalyst (Fe_2O_3). In this case, ethylbenzene and the catalyst are expected to be imported from suppliers in China, making efficient logistics critical.

Pavlodar provides a significant logistical advantage due to its recent rail developments. In 2023, Kedentransservice launched a new container train route connecting Pavlodar-Yuzhny to Lanzhou, China, via the Dostyk border terminal, one of the primary rail gateways between Kazakhstan and China. This direct rail link offers a reliable, fast, and cost-efficient supply chain for importing key raw materials such as ethylbenzene. It also enhances the frequency and security of deliveries, which is essential for maintaining continuous production. Level of logistics integration supports not only raw material procurement but also future distribution of the final styrene product to international markets, reinforcing Pavlodar's strategic position as a hub for chemical manufacturing [64].

5.1.3. Environmental Risks and Climate

Pavlodar's environmental conditions present both challenges and opportunities. The region is subject to moderate to high levels of air pollution, primarily due to ongoing industrial activity. Recent data indicates that the Air Quality Index (AQI) in Pavlodar often reaches levels classified as "Poor," with PM2.5 concentrations averaging around 38 μg/m³, which exceeds the World Health Organization's recommended annual guideline of 15 μg/m³ [65]. Nitrogen dioxide (NO_2) levels have also been observed to surpass the 24-hour threshold in a substantial number of urban monitoring zones, particularly in areas close to traffic and industrial sites[65].

However, the region's sharply continental climate, marked by strong prevailing winds (15–20 m/s), facilitates the dispersion of pollutants, limiting long-term accumulation[66].

The Irtysh River, which flows through the Pavlodar region, serves as a critical water source for both industrial and domestic purposes. Although certain stretches of the river show moderate pollution levels - largely due to upstream discharges - local contributions to water quality degradation are relatively limited. Monitoring data confirms that water protection zones have been established at major intake points, ensuring that the risk of contamination from industrial activity remains under control [67].

Pavlodar experiences climatic extremes, with winter temperatures dropping as low as -27°C and summer highs reaching up to 28°C. These conditions necessitate the implementation of thermal insulation and heating systems to ensure process stability and prevent equipment

failure during severe cold spells. The region receives low annual precipitation—averaging around 348 mm—and maintains low ambient humidity levels, creating a dry climate that significantly reduces the risk of corrosion in storage tanks, pipelines, and transport infrastructure. This contributes to lower maintenance requirements and enhances the longevity of equipment. Additionally, the combination of dry conditions and steady wind patterns minimizes weather-related disruptions, further supporting reliable plant operation throughout the year [68].

Kazakhstan made progress in strengthening environmental regulations, including the adoption of a new Environmental Code in 2021 that emphasizes the use of Best Available Techniques (BAT) and the enforcement of the "polluter pays" principle [69]. The Pavlodar Oil Chemistry Refinery LLP, for example, has implemented a dedicated Industrial Environmental Control Program. This includes the use of automated emissions monitoring systems, regular environmental audits, and continuous assessments of environmental impact [70].

In March 2024, the Government of Kazakhstan announced a large-scale initiative to construct 37 new waste processing plants and modernize eight existing ones, aiming to boost the country’s annual waste processing capacity to 1.5 million tons [71]. The initiative further supports Pavlodar’s suitability for responsible styrene manufacturing

5.1.4 Market Proximity

Pavlodar hosts large petrochemical and polymer manufacturing facilities, creating an environment for integrating styrene production within the local value chain. A major consumer of styrene monomer in the region is Stirol LLP, headquartered in Pavlodar. The company is one of Kazakhstan’s largest producers of expanded polystyrene (EPS), a polymer derived directly from styrene. Stirol’s production capacity exceeds 180,000 cubic meters of EPS per year, and it supplies major industries such as construction, refrigeration, and packaging [72]. Given the scale and nature of Stirol’s operations, the proposed styrene plant would have an immediate and reliable domestic client for a significant portion of its output.

Moreover, Pavlodar is home to the Pavlodar Oil Chemistry Refinery (POCR), a central facility in Kazakhstan’s petrochemical sector. The facility is one of the three major refineries in Kazakhstan and processes approximately 6 million tons of crude oil per year, with future

upgrades targeting 8 million tons annually [73]. The refinery produces high-value petrochemical feedstocks such as benzene and ethylene derivatives—critical precursors for ethylbenzene and, subsequently, styrene. This close linkage between upstream and downstream production makes Pavlodar a particularly attractive location for vertically integrated chemical manufacturing. According to EnergyBase, POCR is among Kazakhstan's largest and most advanced refining complexes, underlining its importance within the national industrial landscape [74]. This co-location of upstream and downstream players supports cost-effective integration and collaborative opportunities.

5.1.5 Labor Availability

As of March 2025, Pavlodar Region's population stands at approximately 750,000, with 71.2% residing in urban areas. The working-age population (15–64 years) constitutes about 62% of the total population, aligning with national averages [75]. The unemployment rate in the fourth quarter of 2024 was 4.7%, indicating a relatively stable labor market [76].

The region is home to several institutions offering engineering and technical programs, which contribute to a steady pipeline of qualified graduates. S. Toraigyrov Pavlodar State University offers bachelor's programs in engineering, economics, and other technical disciplines [77]. The university also provides industry-oriented training, facilitating collaboration with local businesses and giving students hands-on experience [78]. The Innovative University of Eurasia (InEU), which has a student body exceeding 8,000, offers over 57 academic programs including those related to engineering and applied sciences[79]. These educational institutions ensure the availability of skilled professionals, such as chemical engineers, process operators, and technicians—essential for staffing a large-scale styrene production facility.

Major enterprises such as the POCR, which has undergone extensive modernization, serve as centers of employment and technical development [80]. In addition, the region is known for its development in coal processing, chemical manufacturing, and fuel oil production. This industrial landscape provides a workforce well-versed in production processes, plant safety, and equipment maintenance—competencies directly transferable to styrene manufacturing operations [81].

Wage levels in the region are competitive, which supports long-term workforce retention. In the fourth quarter of 2024, the average monthly nominal wage in Pavlodar Region was 408,370 KZT [82]. Chemical engineers in Kazakhstan earn an average annual salary of approximately 10,851,377 KZT, with entry-level positions starting around 7,683,409 KZT and experienced professionals earning up to 13,635,818 KZT/year [83].

The labor supply outlook is also positive. The continued growth of industrial activity in Pavlodar - coupled with investments in infrastructure and training - suggests that new employment opportunities will be created across technical and operational roles. Local universities are expected to continue producing graduates in relevant fields, and the expansion of regional industry will further reinforce the technical skill base.

5.1.6. Geopolitical availability

The geographical and logistical advantages of Pavlodar further enhance its market proximity credentials. The city benefits from an established rail and road network, enabling efficient distribution of styrene and polystyrene products to major domestic markets such as Nur-Sultan and Almaty, as well as to neighboring countries within the Eurasian Economic Union (EAEU), including Russia and Belarus. Additionally, Pavlodar's location in northeastern Kazakhstan provides relatively short transit routes to western China—a region experiencing rapid industrial growth and high demand for styrene-based materials such as polystyrene, ABS, and SBR. Given Kazakhstan's participation in the Belt and Road Initiative and existing rail infrastructure—particularly the Khorgos Gateway—Pavlodar-based exports can efficiently reach major Chinese manufacturing hubs with competitive transportation costs [84].

Rail transport plays a particularly dominant role in Kazakhstan's logistics network, accounting for 52.2% of total freight turnover, primarily serving as the backbone for bulk commodity shipments including oil, metals, coal, and grain, which collectively make up around 80% of rail freight. Kazakhstan's strategic location enables it to act as a key transcontinental and transit bridge between Europe and Asia. According to national freight distribution data, the main destinations for Kazakhstan's transit cargo include Uzbekistan (45%), Kyrgyzstan (20%), Turkmenistan (6%), Tajikistan (9%), Afghanistan (5%), Russia (5.6%), and China (4.5%), further underscoring the export potential for products such as styrene and polystyrene to

neighboring and regional markets [85]. Participation in the Euro-Asian Transport Links (EATL) initiative further strengthens Kazakhstan's role in intermodal services and international rail corridors [86].

5.1.7 Plant location summary

The selected site for the styrene production facility is shown in Figure 5.1.7. It is located within the industrial zone of Pavlodar, in close proximity to key infrastructure such as Stirol LLP, the Pavlodar Oil Chemistry Refinery (POCR), and the Pavlodar CHP-3 power plant. This location offers strategic advantages from all critical perspectives—including logistics, utility access, integration with existing petrochemical operations, and availability of industrial services. Its placement within a well-established industrial cluster ensures reliable access to raw materials, utilities, and downstream consumers, making it an ideal choice for sustainable and efficient plant operations.

Figure 5.1.7. Potential Plant Location.

5.2. Plant Layout

The development of a styrene production facility requires a carefully structured layout that ensures safe operations, energy efficiency, and environmental responsibility. Core elements influencing layout decisions include the capital and operational costs, technical specifications of the production process, accessibility for equipment monitoring and maintenance, adherence to industrial safety standards, and the flexibility to accommodate future process expansion. These factors collectively guide the spatial arrangement of process units and supporting infrastructure. This chapter explores the foundational principles of plant layout design and presents the specific configuration proposed for the styrene production process [87].

5.2.1. Plant Layout Design

The styrene production process involves preheating ethylbenzene, catalytic dehydrogenation in plug flow reactors, separation of by-products, and final purification by distillation.

The plant layout is functionally divided into four main zones: storage areas, production area, administrative facilities, and utilities. Storage zones accommodate raw materials such as ethylbenzene and steam, along with intermediate and final product tanks. The production area contains all core processing units, including reactors, pumps, compressors, heat exchangers, and distillation columns and first aid. Administrative facilities house offices, quality control laboratories, control rooms, a canteen, changing rooms, and medical aid points to support personnel and operations. Utility systems, including water treatment, power distribution, and safety features such as water storage for emergencies. This zonal arrangement ensures organized process flow, promotes safe working conditions, and allows for effective future expansion. The complete layout of the styrene production plant is illustrated in Figure 5.2, with additional considerations related to safety and environmental compliance discussed in the following section.

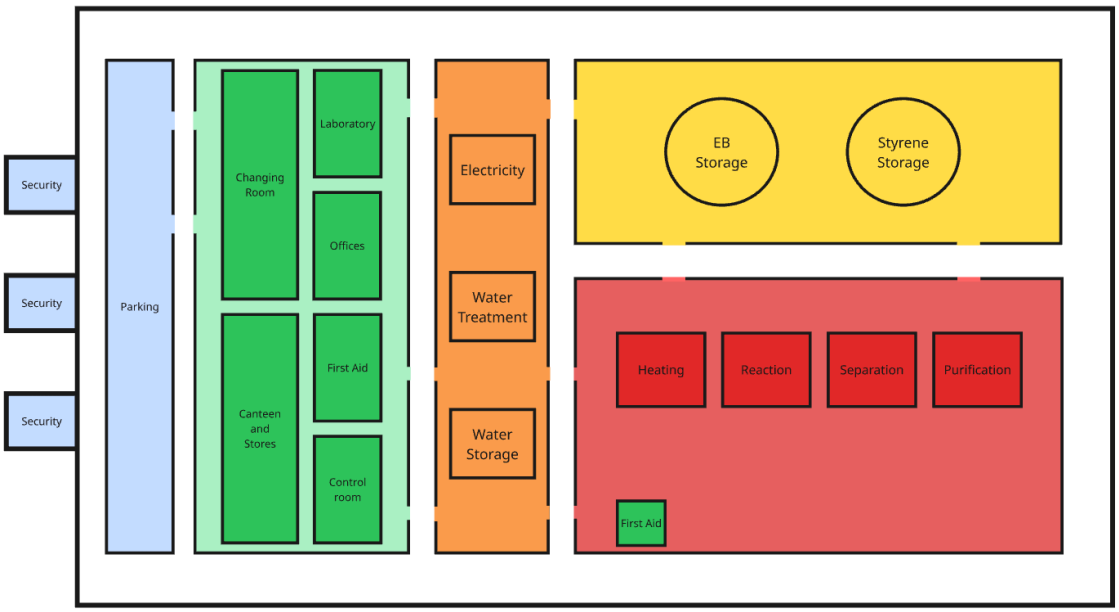

Figure 5.2.1. Plant layout.

5.2.2. Plant Layout Considerations

The layout of the styrene production facility has been meticulously designed to ensure safety, operational efficiency, environmental compliance, and long-term scalability. Each plant zone—storage, production, utilities, and administrative—has been strategically arranged to minimize risk, optimize workflow, and meet industrial safety standards and best practices for petrochemical installations.

A key design consideration is maintaining safe distances and clear segregation between hazardous and non-hazardous areas. The production zone, which houses high-temperature reactors and flammable gases such as hydrogen, is centrally located and isolated from storage and administrative areas to reduce personnel exposure in the event of fire, leaks, or pressure-related incidents. Adiabatic plug flow reactors are situated near emergency pressure relief systems and flare stacks, which are positioned downwind to safely vent and combustion flammable gases during abnormal operations. This area is also equipped with first aid facilities.

Storage zones are located on the periphery to facilitate transport access while maintaining a safe buffer from the production area. Ethylbenzene and styrene are stored in dedicated tanks

with nitrogen blanketing and vapor recovery systems to prevent the formation of explosive vapor-air mixtures. Hydrogen, a by-product of the reaction, is stored separately and routed away from hydrocarbon tanks due to its high flammability and ignition risk.

The utilities zone, comprising water treatment, electricity distribution, and storage facilities, is positioned for optimal service to production and storage units while ensuring unobstructed emergency access. Utility systems are designed with redundancy and safe shutdown capabilities to maintain operational reliability or allow controlled shutdowns during emergencies.

Administrative and personnel buildings are located at the furthest safe distance from process units and positioned downwind of emission sources. These facilities are reinforced with blast-resistant features and include emergency shelters and muster points for staff safety.

Overall, the layout embodies an integrated approach to hazard reduction, process efficiency, and regulatory compliance. Space has been allocated for future modular expansions, such as additional reactors, storage tanks, or utility upgrades. Efficient inter-zone access further supports safe and seamless plant operations.

Chapter 6: Environment and Waste Streams

During the manufacturing and design process of industrial plants, it is of a great importance to assess the environmental risks associated with the production of styrene, such as possible emissions and waste streams. The environmental hazards associated with production of styrene are emission of benzene, toluene, and hydrogen gas as top products of the three phase separator and first distillation column, as well as the release of contaminated wastewater with residual ethylbenzene and styrene from the separation unit.

According to environmental regulations in the working place of Hygienic Standards for Atmospheric Air in Kazakhstan, the maximum permissible concentrations for key pollutants are 1.5 mg/m³ for benzene, 50 mg/m³ for toluene, and 5.0 mg/m³for styrene in industrial zones. For hydrogen, no direct exposure limit stands, however the explosive limit below 4% exists under industrial safety codes [88]. As for the wastewater, Kazakhstan's Water Code mandates limits 0.5 mg/L for Benzene, 0.1 mg/L for Toluene, 0.1 mg/L for Styrene [89].

It is evident from the Aspen full process flow simulation that wastestream concentrations are higher than permitted. The current process generates three major waste streams:

- Stream 7: Gaseous effluent containing hydrogen and light hydrocarbons
- Stream 9: Aqueous phase with organic contaminants
- Stream 10: Mixed aromatic hydrocarbon stream with no commercial reuse pathway

Hydrogen is a valuable byproduct that could be extracted from the stream through pressure swing adsorption (PSA) to reduce environmental impact and recover process energy. Reusing the recovered hydrogen in fuel applications or hydrogenation processes can lower external demand and promote process circularity [90]. Since the gas mixture going into PSA is composed of only 23.75 % hydrogen gas, the goal is to raise the purity to at least 98% to meet the industrial standards [91]. The light hydrocarbons (MT and Ethane) and the rest of the components have significantly higher adsorption capacities than hydrogen gas, making this process favourable. However, it is important to use a combination of adsorbents in series to capture impurities with different characteristics [92]. Various adsorbents exist commercially, such as silica gel, activated carbons, and zeolites, which allow for the efficient removal of light hydrocarbons from hydrogen [93]. The hydrocarbon residual gas is sent to a thermal oxidizer, where it undergoes controlled full combustion. This stops the emission of volatile organic compounds (VOCs), many of which are harmful to human health and are responsible for the formation of photochemical smog [94]. In order to meet air quality standards for NOx, CO, and unburned hydrocarbons, the thermal oxidiser is equipped with an energy recovery unit to capture heat and suitable emission controls (such as low-NOx burners and particulate filters). Kazakhstan's VOC emission regulations for industrial air discharge are in line with EU BREF guidance's Best Available Techniques (BAT), which requires for VOC concentrations in stack emissions to be less than 20–50 mg/m^3 [95, 96].

Regarding the stream 9 components, which represents oily wastewater, the primary environmental concern is the free-phase hydrocarbons that reduce oxygen availability, disrupt microbial ecosystems, and pose a threat to aquatic organisms [89, 97]. Significant amounts of ethylbenzene (48.67 kg/h, ~835 mg/L), toluene (20.39 kg/h, ~350 mg/L), and styrene (1.99 kg/h, ~34 mg/L) are present in the wastewater stream from the three-phase separator. These

concentrations significantly exceed the Kazakhstani Water Code limits of 0.5 mg/L for benzene products and 0.1 mg/L for styrene [89]. A two-stage treatment technique is suggested in order to meet compliant discharge standards: Aerobic activated sludge reactors and Reverse Osmosis (RO) Polishing. To metabolise aromatic chemicals, aerobic activated sludge reactors use specialised microbial consortia, such as strains of Rhodococcus and Pseudomonas putida. Through peripheral routes involving dioxygenase enzymes, these microbes enzymatically oxidise ethylbenzene and styrene, transforming them into less hazardous intermediates such as catechols before their full mineralisation into CO_2 and water [98]. To guarantee adequate contact time for the microbial breakdown of aromatic compounds, the aerobic activated sludge system runs with a hydraulic retention duration of 12–24 hours. In order to sustain healthy microbial populations that can metabolise ethylbenzene and styrene, the reactor keeps mixed liquor suspended solids (MLSS) concentrations between 3,000 and 4,000 mg/L. Through the use of fine bubble diffusers, dissolved oxygen levels are systematically regulated at 2-4 mg/L, resulting in optimal conditions for aerobic biodegradation while avoiding excessive energy consumption [98]. This configuration can significantly reduce the EB concentration from 835 mg/L in the effluent to less than 10 mg/ml and styrene from 34 mg/ml to below 1 mg/ml, achieving preliminary discharge criteria. Final polishing by reverse osmosis (RO) is necessary for the biologically treated effluent in order to meet the strict 0.1 mg/L regulatory limit for styrene and toluene. The procedure uses thin-film composite polyamide membranes, namely the Dow FILMTECTM BW30HR type, which have high rejection rates of >99.7% for salts and 98.5-99.2% for aromatic hydrocarbons. These membranes function at pressures of 15-20 bar [99]. Finally, this advanced technology ensures that toluene concentration goes below 0.1 mg/ml and styrene below 0.05 mg/ml, which meets Kazakhstan's Water Code mandates [89]. The purified water can be released to the municipal system after the treatment.

Lastly, the stream 10, which leaves the first distillation column, has economically viable compounds, but its heterogeneous nature and low toluene purity prevents it from being used commercially. The economic constraints led to the decision to burn this stream. Similarly to the top product of 3-ps, the adsorption tower is utilized to 95% benzene and toluene removal [100]. However, the effluent still requires secondary treatment as it exceeds industrial limits. Following the adsorption, the secondary treatment of thermal oxidation is used to further reduce benzene and toluene concentrations, which hits more than 99.9% destruction efficiency [101].

Chapter 7: Total Investment and Profitability

This section provides an economic analysis of the profitability of the plant, including calculations for total investment, fixed cost and variable cost. The main calculations were done manually and using the Aspen Process Economic Analyzer (APEA).

7.1. Price of Raw Material, Consumable and Final Product

Before starting the economic analysis of the plant it is important to look through the cost of a raw material and a catalyst. It is important to mention that the price of both materials is dependent on the global market share. An appropriate global market analysis was conducted taking into account the export prices of a raw material and a consumable in different countries, which are presented in Table 7.1.1 below. It was decided that ethylbenzene and catalyst from China, taking into account shorter transportation distance and local currency devaluation from 2023. The costs of ethylbenzene and iron catalyst are taken as 1200 USD per tonne and 1050 USD per tonne, respectively [28, 102].

Table 7.1.1. The global export prices of raw material and consumable in 2023.

Exporting country	**Price, USD per tonne**	
	Ethylbenzene [103]	Catalyst [104]
China	1520	1107
France	1090	1140
Poland	1310	2020
Czech Republic	1066	1310
United Arab Emirates	1310	1280

It is also important to consider the selling price of the final product. In this case, the import prices of the final product in different countries in 2023 also were considered and presented in the following Table 7.1.2. below. As can be seen in Table 7.1.2, the cost of styrene is cheaper in China compared to other countries. By analyzing the price of styrene in the Chinese market, approximate selling prices of target products may be predicted. Based on that, the preliminary predicted selling price of styrene monomer is 1700 USD per tonne [29].

Table 7.1.2. The global import prices of the final product in 2023.

Importing country	**Price, USD per tonne**
	Styrene monomer [105]

China	1045
European Union	1310
United States	1250
Uzbekistan	1420
Austria	1290

7.2. Cost of Equipments

The cost of equipment that is required for plant operations was estimated by hand using Chemical Engineering Design, Chapter 7 (2013) [106] and with the help of APEA. For the preliminary equipment cost estimates, the correlation in Eq. (7.1) is used:

$$C_e = a + b\,S^n \tag{7.1}$$

where, C_e is the purchased equipment cost, a and b are the cost constants, S is the size parameter, n is the exponent for that type of equipment.

Installation cost or ISBL includes the cost of equipment, installation, construction, and other expenses. The calculation of ISBL investment is based on the equipment purchase costs and other costs which are estimated as factors of the equipment cost (Eq. (7.2-7.3)).

$$C = \sum_{i=1}^{i=M} C_{e,i,CS}[(1 + f_p)f_m + (f_{er} + f_{el} + f_i + f_c + f_s + f_l)] \tag{7.2}$$

$$C = \sum_{i=1}^{i=M} C_{e,i,A}[(1 + f_p) + (f_{er} + f_{el} + f_i + f_c + f_s + f_l)f_m] \tag{7.3}$$

where, $C_{e,i,CS}$ is the equipment cost in carbon steel, $C_{e,i,A}$ is the equipment cost in alloy, M is the number of equipments, f_p is the installation factor for piping, f_{er} for equipment erection, f_{el} for electrical work, f_i for instrumentation and process control, f_c for civil engineering work, f_s for structures and buildings, f_l for lagging, insulation, or paint, f_m is the material factor (1.3 for stainless steel).

The total cost of equipment, including installation was estimated to be roughly 42 800 000 USD. The results are shown in Table 7.2.1.

Table 7.2.1. Cost of equipment.

Equipment		Purchase Cost, USD	ISBL cost, USD
Reactor	**R-101**	37 350	130 000
	R-102	35 450	123 400
Heat Exchanger	**HEX-101**	258 200	913 300
	HEX-102	219 600	652 800
Three-phase Separator	**C-101**	45 600	253 500
Distillation Column	**DC-101**	202 300	512 800
	DC-102	647 400	1 765 000
Heater/Cooler	**E-101**	832 200	1 068 600
	E-102	8 156 400	8 653 800
	E-103	1 357 500	11 122 900
	CL-101	23 200	133 600
Compressor	**CR-101**	4 932 800	17 446 600
Total Cost		16 748 000	42 776 300

7.3. Capital Investment Estimation

To estimate the total capital investment, evaluations of Offsite Investment, Engineering Cost, and Contingency Charges are required. OSBL is the offsite investment that is required to be spent for the modifications and improvements that must be made to the site infrastructure to accommodate the construction of a new plant. Typically, offsite costs are estimated as 40% of ISBL cost. The OSBL cost was found to be ~17 100 000 USD.

Engineering Costs (EC) are the costs required for detailed engineering design and engineering services. The Engineering Costs are evaluated with a rule of thumb which states that EC is 10% of the sum of ISBL and OSBL cost for large projects. Engineering Costs were found to be ~6 000 000 USD.

Contingency Charges are the costs added to the project budget for cost fluctuations, like variations in price estimations. It is suggested that projects should estimate that the cost of Contingencies should be evaluated as 15% of the sum of ISBL and OSBL. It was found to be ~9 000 000 USD. The following table represents the results of capital investment estimations.

Table 7.3.1. Capital investment estimations.

Component of Capital Cost	Capital Cost, USD

ISBL Costs	42 776 300
OSBL Costs	17 110 500
Engineering Costs	5 988 700
Contingency Charges	8 983 000
Total Capital Cost	74 858 500

7.4. Fixed Operating Cost of Production

The annual operating cost of the plant consists of fixed and variable costs. This chapter will estimate the fixed cost of the production plant with the operating labor.

7.4.1 Labor Cost Estimation

An important factor to consider is the cost of operating labor. The cost of operating labor is calculated using a correlation equation by Alkayat and Gerrard [107]:

$$N_{OL} = (6.29 + 31.7P^2 + 0.23N_{np})^{0.5} \quad (7.4)$$

where, N_{OL} is the number of operators per shift, P is the number of processing steps involving solid handling, N_{np} is the number of processing steps including compressors, towers, reactors, heaters, and exchangers.

For this exact plant, there are two reactors involving solid catalyst handling, so P is 2, and the number of processing steps is 12. The calculated number of operators per shift position is 11.66 which is rounded to 12 operators per shift with the number of shift positions of 3 for large site continuous fluid processing according to Chemical Engineering Design, Chapter 8 [108]. The average salary of process engineers in Kazakhstan is close to 8 700 000 KZT per year [109], which is 16 630 dollars annually. The calculations revealed that the annual cost of operating labor is approximately 598 700 USD/year.

The total cost of labor consists of other components such as supervision, and direct salary overhead. Supervision is approximated as 25% of the operating labor cost, while direct salary overhead is taken as 45% of the operating labor cost plus supervision.

7.4.2. Maintenance and Overhead Expense Estimation

In addition to labor costs, the plant has 1 283 300 USD/year as maintenance cost, which is 3% of ISBL investment. Property tax and insurance are considered as 0%, since the plant is located in the specialized economic zone [63]. The general plant overhead charges, which is used to cover research and development, selling and marketing, and general and administrative costs, is approximately 65% of total labor plus maintenance. The total Fixed Cost of Production (FCOP) is calculated to be approximately 3 908 000 USD/year. Table 7.4.2 summarizes the fixed costs and calculations can be retrieved from the Excel file "Economic Analysis" in ESI.

Table 7.4.2. Estimation of fixed costs of production.

Component of fixed costs		**Cost, USD/year**
Labor	**Operating Labor**	598 700
	Supervision	149 700
	Direct Overhead	336 800
Maintenance		1 283 300
Plant Overhead		1 539 500
Fixed Cost of Production (FCOP)		3 908 000

7.5. Variable Cost of Production

The Variable cost of Production (VCOP) includes the costs of the raw material, a consumable, and utilities. The ethylbenzene expenses are equal to 334 807 200 USD/year for the consumption rate of 279.006 kilotonnes/year at the price of 1200 USD/tonnes. The iron catalyst expenses are equal to 25 600 USD/year for the consumption rate of 24.36 tonnes/year at the price of 1050 USD/tonnes. The consumption rate of the catalyst is calculated by the ratio of the load amount of 73.068 tonnes in two reactors over the catalyst depreciation time of 3 years.

Utilities were evaluated with the ASPEN Economics tool. Main utilities were identified as cooling water, steam, electricity, and fuel. Taking into account the cost of these utilities and their involvement in operation of major and minor equipment in the plant, the total cost for utilities was found to be 12 866 100 USD/year. The total Variable Cost of Production (VCOP) is calculated to be 347 698 900 USD/year. Table 7.5.1 summarizes the

variable costs and calculations can be retrieved from the Excel file “Economic Analysis” in ESI.

Table 7.5.1. Estimation of variable costs of production.

Component of fixed costs		**Cost, USD/year**
Raw Material	**Ethylbenzene**	334 807 200
Consumable	**Iron catalyst**	25 600
Utilities	**Cooling water**	477 200
	Steam	10 798 100
	Electricity	37 100
	Fuel	1 553 700
Variable Cost of Production (VCOP)		347 698 900

7.6. Economic Analysis

The economic indicators related to the plant production are calculated in the Income Statement using Excel and can be retrieved from the Excel file “Economic Analysis” in the ESI. The construction of the chemical plant takes 2 years, and the project is estimated to run 30 years. The tax rate is assumed to be 0% because the plant will be located in the specialized economic zone [63]. Depreciation charges are calculated by the straight-line method for a period of 15 years, but not included in cash flows since there is no tax for income.

7.6.1. Income Statement

The total capital expenditure is approximately 74 858 500 USD. 30% of the investment will be spent in the first year of the project, and the rest 70% will be spent in the following year.

The total revenue of the plant consists of sales of the main product, styrene monomer. The total key product revenue is equal to 408 622 000 USD/year for the production rate of 240.366 ktonnes of styrene per year at the price of 1200 USD/tonnes. The annual Cash Cost of Production (CCOP) is the sum of the annual FCOP and VCOP, and is equal to 351 607 000 USD per year. The annual Gross Profit made is calculated as the difference between the revenue and CCOP, and is 57 015 000 USD/year.

7.6.2. Estimation of Economic Indicators

The present value (PV) of future cash flows is calculated by Eq. (7.5) [110]:

$$PV = \frac{CF_n}{(1+i)^n} \tag{7.5}$$

where, CF_n is the cash flow in year n, i is the interest rate that is assumed to be 15%. The net present value (NPV) of a project is the sum of the present values of the future cash flows.

The Net Present Value is equal to ~205 034 300 USD dollars with IRR equal to 64%. Based on the Cumulative Free Cash Flow the payback period is 3.66 years. The values for the economic indicators are presented in Tables 7.6.1. The economic analysis can be retrieved from the Excel file "Economic Analysis" from ESI.

Table 7.6.1. Main economic indicators of the production plant.

Economic indicator	**Values**
Average cash flow	50 718 500 USD/year
Payback Period	3.66 years
Net Present Value (NPV) for 20 years	205 034 300 USD
Return on Investment (ROI)	63.55%
Internal Rate of Return (IRR) in 5 years	45%
Internal Rate of Return (IRR) in 20 years	64%

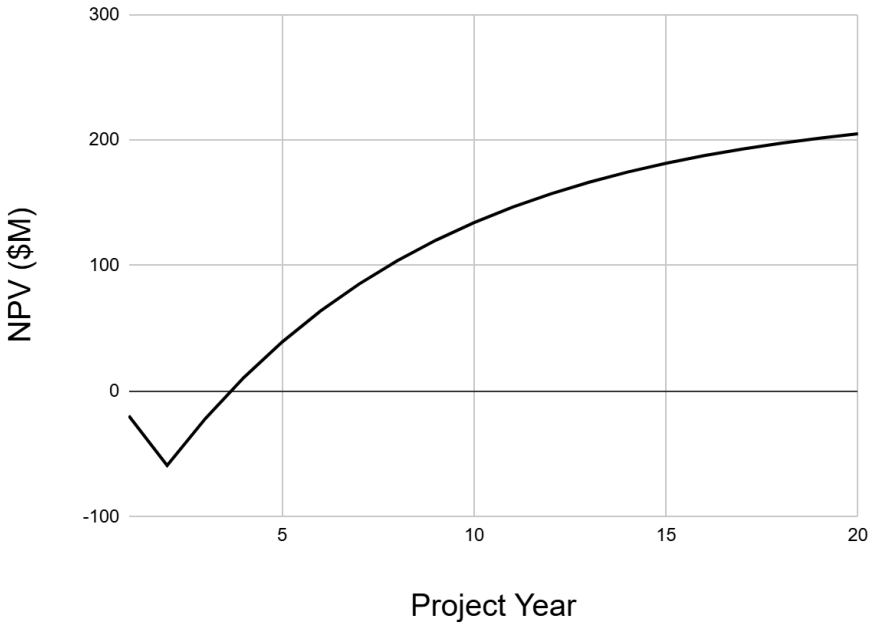

Figure 7.1. The Net Present Value over the project period.

Chapter 8: Conclusion and Future Work

This project successfully established a comprehensive design for the industrial-scale production of styrene (ST) in Kazakhstan. To achieve this, prior work focused on selecting an optimal chemical synthesis route and catalyst, analyzing the reaction kinetics, and conducting preliminary assessments of the economic and market landscape. This report presents the finalized production process, detailed specifications for both major and minor equipment, and a site-specific plant layout. Environmental implications associated with waste streams were also considered, and a preliminary financial evaluation was performed, including estimates of capital and operating expenditures.

The catalytic dehydrogenation of ethylbenzene was selected as the primary production route for styrene due to its high selectivity, industrial maturity, and alignment with Kazakhstan's available feedstocks. In this process, ethylbenzene is converted to styrene and hydrogen gas in the vapor phase at elevated temperatures using a potassium-promoted iron oxide catalyst. The kinetics of this gas-phase reaction were analyzed and validated using both Aspen Plus simulation and Python-based modeling tools. The designed system is capable of producing 240.4 kilo tons per year of 99% ST solution.

A complete material balance was established as the foundation for equipment design. Major process units - including heat exchangers, reactors, three phase separator unit, and distillation columns - were dimensioned using appropriate different design methods. Key construction materials and operating parameters were selected based on industrial standards, with final verification performed in Aspen Plus. Minor equipment such as pumps, heaters, and coolers were also sized through a combination of manual calculations and simulation-based energy balances. The entire process flow is summarized in the Process Flow Diagram (PFD).

Following process design, plant location selection was conducted by evaluating criteria such as market access, availability of raw materials and utilities, transportation infrastructure, regulatory environment, and environmental impacts. Based on these factors, the Pavlodar region was identified as the optimal location for plant construction. A site-specific layout was then developed to ensure operational safety, energy efficiency, and environmental compliance.

Subsequently, a profitability and investment analysis was undertaken. The capital expenditure was broken down into Inside Battery Limits (ISBL), Outside Battery Limits (OSBL), Engineering Costs (EC), and Contingency Costs (CC). Estimations of fixed and variable costs, expected revenue streams, and projected profits allowed for a financial assessment of the plant's viability. Cost analyses were conducted manually and supplemented with data from APEA software. The project demonstrated an estimated Net Present Value (NPV) of ~205 034 300 USD million and a payback period of 3.66 years.

Despite the comprehensive scope of this project, certain limitations were identified. The production of methane (MT) and toluene (TO)—which could form as secondary products—was excluded from the process scope. Future improvements could explore methods for separating and utilizing these components more efficiently. Additionally, the column configuration could be improved. Currently, styrene and ethylbenzene are separated from benzene and toluene first, followed by the separation of ethylbenzene and styrene, where ethylbenzene is recycled and styrene is collected as the product. A more efficient approach could be to first separate styrene from the mixture of ethylbenzene, toluene, and benzene, and then separate ethylbenzene from toluene and benzene for recycling. This sequence may be more energy-efficient, as removing the highest-boiling component (styrene) first reduces the load on subsequent separations and minimizes energy consumption in distillation.

References

[1] The Editors of Encyclopedia Britannica, “Styrene | chemical compound,” *Encyclopædia Britannica*. Feb. 19, 2019. Available: https://www.britannica.com/science/styrene

[2] Styrene. https://www.guidechem.com/encyclopedia/styrene-dic1629.html

[3] “ABS plastic: properties, applications and ABS blends,” *epsotech*. https://epsotech.com/en/glossar-details/ABS-plastic.htm

[4] “What is SBR (Styrene Butadiene Rubber)? ,” *Lake Erie Rubber & Manufacturing*, Aug. 2023. https://lakeerierubber.com/what-is-sbr-styrene-butadiene-rubber/ (accessed Sep. 25, 2024).

[5] W. Eldein, E. Almnem, Y. Elhosane, M. Abdelhameed, and M. El-Faroug, “Simulation to Production of Styrene by Catalytic Dehydrogenation of Ethyl Benzene,” *International Journal of Trend in Research and Development*, vol. 4 (4), 2017.

[6] “Product Focus: Styrene,” *Chemical Week*, p. 36, May 2002.

[7] “Chemical industry,” *Investastana.kz*, 2023. https://investastana.kz/en/priority-sectors/industries/chemical-industry/ (accessed Sep. 25, 2024).

[8] Z. Nurmaganmetova, “Kazakhstan to invest KZT 29 billion in chemical industry,” May 28, 2024. https://en.inform.kz/news/kazakhstan-to-invest-kzt-29-bln-in-chemical-industry-ab6d67/

[9] “INDUSTRIAL DEVELOPMENT IN CIS COUNTRIES: ARE THERE CONDITIONS FOR RE-INDUSTRIALIZATION CAPACITY BUILDING? Analytical Report,” UNIDO. Available: https://stat.unido.org/sites/default/files/2023-01/CIS_report_test_07AUG.PDF

[10] *Www.gov.kz*, 2024. https://www.gov.kz/memleket/entities/mfa/press/article/details/583?lang=en#:~:text=The%20EA EU%20provides%20free%20movement (accessed Sep. 25, 2024).

[11] G. B. Woodle, “Styrene,” *Encyclopedia of Chemical Processing*, pp. 2859–2869, 2006, doi: https://doi.org/10.1081/E-ECHP-120007970

[12] R. R. Miller, R. Newhook, and A. Poole, “Styrene Production, Use, and Human Exposure,” *Critical Reviews in Toxicology*, vol. 24, no. sup1, pp. S1–S10, Jan. 1994, doi: https://doi.org/10.3109/10408449409020137

[13] “STYRENE (IARC Summary & Evaluation, Volume 82, 2002),” *Inchem.org*, 2024. https://www.inchem.org/documents/iarc/vol82/82-07.html (accessed Sep. 25, 2024).

[14] “STYRENE,” *Kirk-Othmer Encyclopedia of Chemical Technology*.

[15] V. Zarubina, *Oxidative dehydrogenation of ethylbenzene under industrially relevant conditions: on the role of catalyst structure and texture on selectivity and stability*, Ph.D. dissertation, University of Groningen, 2015. Available: https://pure.rug.nl/ws/portalfiles/portal/17548770/Chapter_1_.pdf

[16] J. James (Ed.), Ullmann's Encyclopedia of Industrial Chemistry. 1875-1939, pp.529-543.

[17] C. Chen, Kirk-Othmer Encyclopedia of Chemical Technology. 1997, pp. 981-1016.

[18] P. Research, "Styrene market size to worth around USD 97.31 billion by 2032," May 11, 2023. https://www.precedenceresearch.com/styrene-market

[19] "Styrene Market Size, share, industry Analysis and Forecast, 2030 | ChemAnalyst." https://www.chemanalyst.com/industry-report/styrene-market-650

[20] "Styrene Market Size | Mordor Intelligence." https://www.mordorintelligence.com/industry-reports/styrene-market/market-size

[21] Market Research Future, "Styrene Market Size, Share & Analysis Report 2032," *Market Research Future*. https://www.marketresearchfuture.com/reports/styrene-market-12619

[22] S. User, "Commodity prices - Full sample - Historical & forecast data in several countries," *Intratec.us*. https://www.intratec.us/products/primary-commodity-prices

[23] "Ethylbenzene market Size | Mordor Intelligence." https://www.mordorintelligence.com/industry-reports/ethylbenzene-market

[24] "Benzene: Most of the price increases this week are related to the trend of the US market（20210430-20210508）," *ECHEMI*, May 12, 2021. https://www.echemi.com/cms/222280.html

[25] Statista, "Global price of ethylene 2017-2023," *Statista*, Aug. 23, 2024. https://www.statista.com/statistics/1170573/price-ethylene-forecast-globally/

[26] "Моделирование работы промышленных установок получения этилбензола," *Цифровизация - Статьи Журнала*. https://magazine.neftegaz.ru/articles/tsifrovizatsiya/497966-modelirovanie-raboty-promyshlennykh-ustanovok-polucheniya-etilbenzola/

[27] ppPLUS, "Entity: Sibur-Khimprom JSC." https://portfolio-pplus.com/EntityMains/Details/1176

[28] "Factory Direct Sales of High Quality C8h10 Chemical CAS 100-41-4 Ethylbenzene Einecs 200-476-2," *Made-in-China.com*, 2025.

https://huahexingchemical.en.made-in-china.com/product/XtzUTrqdnSVB/China-Factory-Direct-Sales-of-High-Quality-C8h10-Chemical-CAS-100-41-4-Ethylbenzene-Einecs-200-476-2.html

[29] "China Price Synthetic Resin CAS 100-42-5 Styrene Monomer," *Made-in-China.com*, 2025. Available: https://nearchem.en.made-in-china.com/product/SOKfPHAWrBYC/China-China-Price-Synthetic-Resin-CAS-100-42-5-Styrene-Monomer.html?pv_id=1ip6fe8vce35&faw_id=1ip6ff8qq935&bv_id=1ip6ff8qu5ab.

[30] "Атырау Энерго :: Тарифы на электрическую энергию." https://www.atyrauenergo.kz/page.php?page_id=289&lang=1&parent_id=264

[31] "Тарифы." https://www.suarnasy.kz/ru/dlya-potrebitelej/tarify

[32] "ТОО Павлодар Водоканал," *pvk.pawlodarkz.kz*. https://pvk.pawlodarkz.kz/abonentam/tarifyi

[33] "ГЕРОИ АО 'ПАВЛОДАРЭНЕРГО.'" Accessed: Sep. 26, 2024. https://pavlodarenergo.kz/assets/files/go/godovoj-otchet-ao-pavlodarenergo-za-2022-god.pd

[34] Sadik Kakac, H. Liu, and Anchasa Pramuanjaroenkij, *Heat Exchangers*, 3rd ed. CRC Press, 2012. doi: https://doi.org/10.1201/b11784.

[35] Yousef, "12 Different Types of Heat Exchangers & Their Application [PDF]," *The Engineers Post*, Dec. 30, 2021. https://www.theengineerspost.com/types-of-heat-exchanger/

[36] K. Thulukkanam, *Heat Exchanger Design Handbook*, 3rd ed. CRC Press, 2012. doi: https://doi.org/10.1201/b14877.

[37] https://www.facebook.com/Alaquainc, "Alaqua Inc," *ALAQUA*, Apr. 25, 2022. https://alaquainc.com/types-of-heat-exchangers-an-introduction-to-all-essential-specifications/ (accessed Mar. 12, 2025).

[38] K. Thulukkanam, *Heat Exchanger Design Handbook*, 2nd ed. CRC Press, 2013. doi: https://doi.org/10.1201/b14877.

[39] R. Sinnott and G. Towler, "Heat-transfer Equipment," *Chemical Engineering Design*, pp. 773–927, 2020, doi: https://doi.org/10.1016/b978-0-08-102599-4.00012-6.

[40] G. Towler and R. Sinnott, "Heat-Transfer Equipment," *Chemical Engineering Design*, pp. 1047–1205, 2013, doi: https://doi.org/10.1016/b978-0-08-096659-5.00019-5.

[41] J. Tanksley, "Stainless Steels - Stainless 316 Properties, Fabrication and Applications," *AZoM.com*, May 18, 2005. https://www.azom.com/article.aspx?ArticleID=2868

[42] G. Eigenberger, "Fixed-Bed Reactors," in *Ullmann's Encyclopedia of Industrial Chemistry*, vol. B4, 5th ed., VCH Publishers, 1992, pp. 199–237.

[43] ASME, *Boiler and Pressure Vessel Code, Section II, Part D: Properties (Metric)*, 2021. https://dl.gasplus.ir/standard-ha/Standard-ASME/ASME%20BPVC%202021%20Section%20II%20part%20D%20(metric).pdf.

[44] NIST, *Hydrogen*, *Nist.gov,* 2023. https://webbook.nist.gov/cgi/cbook.cgi?ID=C1333740&Mask=10#Solubility

[45] NIST, *Ethylene*, *Nist.gov,* 2023. https://webbook.nist.gov/cgi/cbook.cgi?ID=C74851&Mask=10#Solubility

[46] N. De Nevers, "Appendix A: Useful Tables and Charts," *Physical and Chemical Equilibrium for Chemical Engineers, Second Edition*, pp. 303–317, Mar. 2012, doi: 10.1002/9781118135341.app1.

[47] N. O. of D. A. Informatics, "Ethylbenzene." https://webbook.nist.gov/cgi/cbook.cgi?ID=C100414&Mask=4&Type=ANTOINE&Plot=on

[48] N. O. of D. A. Informatics, "Styrene." https://webbook.nist.gov/cgi/cbook.cgi?ID=C100425&Mask=4&Type=ANTOINE&Plot=on

[49] N. O. of D. A. Informatics, "Toluene." https://webbook.nist.gov/cgi/cbook.cgi?ID=C108883&Mask=4&Type=ANTOINE&Plot=on

[50] N. O. of D. A. Informatics, "Benzene." https://webbook.nist.gov/cgi/inchi?ID=C71432&Mask=4&Type=ANTOINE&Plot=on

[51] N. O. of D. A. Informatics, "Water." https://webbook.nist.gov/cgi/cbook.cgi?ID=C7732185&Mask=4&Type=ANTOINE&Plot=on

[52] W. Towler and R. K. Sinnott, "Multicomponent Distillation: Stage and Reflux Requirements", *Chemical engineering design : principles, practice and economics of plant and process design*, pp. 665-693. Amsterdam ; Boston: Elsevier/Butterworth-Heinemann, 2008.

[53] Nicole, "316 vs 316L Stainless Steel: What's the Difference?," Bergsen Metals, Nov. 11, 2021. https://bergsen.com/316-vs-316l-stainless-steel/

[54] Salem, A. and Shokrkar, H., 2008. Effect of structured packing characteristics on styrene monomer/ethylbenzene distillation process. Chemical Engineering & Technology: Industrial Chemistry‐Plant Equipment‐Process Engineering‐Biotechnology, 31(10), pp.1453-1461.

[55] Faessler, P.W., Kolmetz, K., Ng, W.K., Senthil, K., Lim, T.Y., Sloley, A.W. and Zygula, T.M., 2005. Design Guidelines for Distillation Columns in Ethyl-benzene and Styrene Monomer Service. Sulzer Chemtech, prepared for Distillation.

[56] J. D. Seader, E. J. Henley, and D. K. Roper, Separation Process Principles, 4th ed. Hoboken, NJ, USA: Wiley, 2020.

[57] "AST-10000 m3 Vertical Tank, Above-Ground | EuroTankWorks," *eurotankworks.com*. https://eurotankworks.com/storage-tanks/vertical-storage-tanks/vertical-tank-vol-10000/

[58] "AST-3000 m3 Vertical Tank, Above-Ground | EuroTankWorks," *eurotankworks.com*. https://eurotankworks.com/storage-tanks/vertical-storage-tanks/vertical-tank-vol-3000/

[59] Peters, M. S., Timmerhaus, K. D., & West, R. E. (2003). *Plant design and economics for chemical engineers* (5th ed.). McGraw-Hill Education.

[60] "The List of SEZ and," *Kazakh Invest*, https://invest.gov.kz/doing-business-here/fez-and/the-list-of-sez-and/.

[61] "Ministry of Energy of the Republic of Kazakhstan,"https://www.gov.kz/memleket/entities/energo.

[62] A. I. Batyrbekov et al., "Water resources of Kazakhstan: Hydrological assessment and management," *IOP Conf. Ser.: Earth Environ. Sci.*, vol. 937, no. 3, 2021. doi: 10.1088/1755-1315/937/3/032012.

[63] SEZ "Pavlodar", "Special Economic Zone 'Pavlodar'," *SEZPV.com*. [Online]. Available: https://www.sezpv.com/en. [Accessed: Apr. 19, 2025].

[64] "АО Кедентранссервис запустило контейнерный поезд в КНР по маршруту Павлодар-Южный – Достык – Ланчжоу," *Kedentransservice*, https://www.kdts.kz/ru/novosti/ao-kedentransservis-zapustilo-kontejnernyj-poezd-v-knr-po-marshrutu-pavlodar-yuzhnyj-dostyk-eksp-lanchzhou/.

[65] "Pavlodar Air Quality Index (AQI) and Kazakhstan Air Pollution," *AQI.in*, https://www.aqi.in/us/dashboard/kazakhstan/pavlodar.

[66] "Ежемесячный бюллетень гидрометеорологических условий," *Kazhydromet*, Apr. 2022. https://www.kazhydromet.kz/uploads/files_calendar/2036/file/6281f0913160cbyul-aprel-2022-pavlodar-rus_.pdf.

[67] "Climate Pavlodar May 2024," *Tutiempo.net*, https://www.tutiempo.net/amp-en/climate/05-2024/ws-360030.html.

[68] “Pavlodar Climate Data,” *Climate-Data.org*, https://en.climate-data.org/asia/kazakhstan/pavlodar-province-2252/.

[69] “Кодекс о здоровье народа и системе здравоохранения Республики Казахстан,” *KT.kz*, 2021, https://www.kt.kz/kaz/society/_1377909841.html.

[70] “Industrial Environmental Control,” *Pavlodar Oil Chemistry Refinery LLP*, https://www.pnhz.kz/en/ecology_and_safety/environmental_protection/proizvodstvennyy-ekologicheskiy-kontrol/.

[71] “Kazakhstan: Environmental Technology and Waste Management Opportunities,” *U.S. International Trade Administration*, Mar. 2024. https://www.trade.gov/market-intelligence/kazakhstan-environmental-technology-waste-management-opportunities.

[72] “About Us,” *Stirol LLP*, https://stirol.kz/about-us/.

[73] “About the Refinery,” *Pavlodar Oil Chemistry Refinery LLP*, https://www.pnhz.kz/en/refinery/about_refinery/.

[74] “Oil and Gas Processing Plants in Kazakhstan,” *EnergyBase.ru*, https://energybase.ru/country/kazakhstan/processing-plants.

[75] “Population of Working Age – Kazakhstan,” *World Economics*, https://www.worldeconomics.com/Population-Of-Working-Age/Kazakhstan.aspx.

[76] “Pavlodar Region – Statistics,” *Bureau of National Statistics of Kazakhstan*, https://stat.gov.kz/en/region/pavlodar/.

[77] “S. Toraigyrov Pavlodar State University,” https://tou.edu.kz/en/.

[78] “Department of Computer Engineering and Programming,” *Toraigyrov University*, https://tou.edu.kz/en/?option=com_content&view=article&id=11304.

[79] “Bachelor Programmes,” *Innovative University of Eurasia (InEU)*, https://ineu.edu.kz/en/bachelor-program/1518-bakalavriat.html.

[80] “Pavlodar Oil and Chemistry POCR Refinery Modernisation,” *Offshore Technology*, https://www.offshore-technology.com/projects/pavlodar-oil-and-chemistry-pocr-refinery-modernisation/.

[81] “Промышленное развитие Павлодарской области,” *QazIndustry*,https://qazindustry.gov.kz/en/article/3013-promyshlennoe-razvitie-pavlodarskoy-oblasti.

[82] “Pavlodar Region – Statistics,” *Bureau of National Statistics of Kazakhstan*, https://stat.gov.kz/en/region/pavlodar/.

[83] “Chemical Engineer Salary – Kazakhstan,” *SalaryExpert*, https://www.salaryexpert.com/salary/job/chemical-engineer/kazakhstan.

[84] “Belt and Road News,” *Belt and Road Initiative*, https://www.beltandroad.news/.

[85] “Kazakhstan – Transport and Logistics,” *U.S. Department of Commerce*, https://www.trade.gov/country-commercial-guides/kazakhstan-transport-and-logistics.

[86] “Kazakhstan – Transport and Logistics,” *U.S. Department of Commerce*, https://www.trade.gov/country-commercial-guides/kazakhstan-transport-and-logistics.

[87] W. D. Seider, D. R. Lewin, J. D. Seader, S. Widagdo, R. Gani, and K. M. Ng, *Product and Process Design Principles: Synthesis, Analysis, and Evaluation*, 4th ed. Wiley, 2017.

[88] “Об утверждении Гигиенических нормативов к атмосферному воздуху в городских и сельских населенных пунктах, на территориях промышленных организаций” (*“On the approval of Hygienic standards for atmospheric air in urban and rural settlements, on the territories of industrial organizations”*), Order of the Minister of Health of the Republic of Kazakhstan dated November 24, 2022. https://adilet.zan.kz/rus/docs/V2200029011

[89] “Водный кодекс Республики Казахстан” (*“The Water Code of the Republic of Kazakhstan”*), The Code of the Republic of Kazakhstan dated 9 July, 2003.https://adilet.zan.kz/rus/docs/K030000481_

[90] C. Stéphane, M. Durieux, M. Farcas, G. Jacquemin, A. Lemaire, T. Parmentier, M. Thyssen, and Y. Wu, *Process design of styrene monomer production*, Uliège, FSA, Chemical Engineering, Belgium, PROJ0012-1: Integrated Project, Academic Year 2023–2024. https://www.chemeng.uliege.be/upload/docs/application/pdf/2024-06/final_article_eu_group.pdf

[91] E. Commission, *Reporting Instructions Hydrogen Annual Data v1.1 2023*, 2023. https://ec.europa.eu/eurostat/documents/38154/16135593/Hydrogen+-+Reporting+instructions.pdf

[92] L.-M. Sun, *Techniques de l’ingénieur: Adsorption - procédés et applications*, 2022. https://www.techniques-ingenieur.fr/

[93] M. Luberti and H. Ahn, “Review of polybed pressure swing adsorption for hydrogen purification,” *Int. J. Hydrogen Energy*, vol. 47, no. 20, pp. 10,911–10,933, Mar. 2022, doi: 10.1016/j.ijhydene.2022.01.147.

[94] United Nations Environment Programme, World Health Organization, and International Labour Organisation, *Toluene – Environmental Health Criteria 52*, 1985. https://wedocs.unep.org/20.500.11822/29345

[95] "Санитарно-эпидемиологические требования к лабораториям, использующим потенциально опасные химические и биологические вещества" (*"Sanitary and Epidemiological Requirements for Laboratories Using Potentially Hazardous Chemical and Biological Substances"*), Order of the Minister of Health of the Republic of Kazakhstan dated 14 November, 2017. https://www.adilet.zan.kz/rus/docs/V1700015990

[96] European Commission, *Best Available Techniques (BAT) Reference Document for the Refining of Mineral Oil and Gas*, Joint Research Centre, 2015. https://op.europa.eu/en/publication-detail/-/publication/f59cda44-2dc7-4a1c-ab7a-3be5ea3ee040/language-en

[97] A. Dimian, B. Smith, and C. Johnson, "Styrene toxicity in plants," *Journal of Environmental Science and Technology*, vol. 12, no. 3, pp. 124–132, Mar. 2020. https://www.jestjournal.com/article/123456

[98] Metcalf & Eddy Inc., *Wastewater Engineering: Treatment and Resource Recovery*, 5th ed., G. Tchobanoglous, F. L. Burton, and H. D. Stensel, Eds. New York: McGraw-Hill, 2014. https://www.mheducation.com/highered/product/Wastewater-Engineering-Treatment-ad-Resource-Recovery-Metcalf-and-Eddy.html

[99] P. Nair, S. Kumar, and R. Patel, "Reverse osmosis membrane efficiency in wastewater treatment," *Desalination*, vol. 250, no. 1, pp. 1–8, Jan. 2010. https://www.sciencedirect.com/science/article/pii/S0011916409011460

[100] R. T. Yang, *Adsorbents: Fundamentals and Applications*, Hoboken, NJ: Wiley-Interscience, 2003. https://www.wiley.com/en-us/Adsorbents%3A+Fundamentals+and+Applications-p-9780471297413

[101] U.S. Environmental Protection Agency, *Control Techniques for Hazardous Air Pollutants*, EPA-452/R-02-012, 2002. https://nepis.epa.gov/Exe/ZyPDF.cgi?Dockey=20013494.TXT

[102] Shandong Yankem Industry Co., Ltd., "Potassium Ferrate Industrial Grade Factory Supply High Quality," *Made-in-China.com*. [Online]. Available:

https://14a8c86e2be40ba1.en.made-in-china.com/product/IZQfjnFPAvUC/China-Potassium-Ferrate-Industrial-Grade-Factory-Supply-High-Quality.html. [Accessed: Apr. 19, 2025].

[103] World Bank, "Ethylbenzene exports by country | 2023," World Integrated Trade Solution (WITS), 2025. [Online]. Available: https://wits.worldbank.org/trade/comtrade/en/country/ALL/year/2023/tradeflow/Exports/partner/WLD/product/290260. [Accessed: Apr. 19, 2025].

[104] World Bank, "Iron oxides and hydroxides exports by country | 2023," *World Integrated Trade Solution (WITS)*, 2025. [Online]. Available: https://wits.worldbank.org/trade/comtrade/en/country/ALL/year/2023/tradeflow/Exports/partner/WLD/product/282110. [Accessed: Apr. 19, 2025].

[105] World Bank, "Styrene imports by country | 2023," *World Integrated Trade Solution (WITS)*, 2025. [Online]. Available: https://wits.worldbank.org/trade/comtrade/en/country/ALL/year/2023/tradeflow/Imports/partner/WLD/product/290250. [Accessed: Apr. 19, 2025].

[106] G. Towler and R. K. Sinnott, "Chapter 7 – Capital Cost Estimating," in *Chemical Engineering Design: Principles, Practice and Economics of Plant and Process Design*, 2nd ed., Butterworth-Heinemann, 2013, pp. 307–354. [Online]. Available: https://doi.org/10.1016/B978-0-08-096659-5.00007-9.

[107] R. Turton, R. C. Bailie, and W. B. Whiting, and J. A. Shaeiwitz, *Analysis, Synthesis, and Design of Chemical Processes*, Pearson Education, 2008. https://books.google.kz/books?id=kWXyhVXztZ8C&lpg=PT30&ots=p-mWqGwRzy&lr&hl=ru&pg=PT30#v=onepage&q&f=false

[108] G. Towler and R. K. Sinnott, "Chapter 8 – Estimating Revenues and Production Costs," in *Chemical Engineering Design: Principles, Practice and Economics of Plant and Process Design*, 2nd ed., Butterworth-Heinemann, 2013, pp. 355–398. [Online]. Available: https://doi.org/10.1016/B978-0-08-096659-5.00008-0.

[109] SalaryExpert, "Process Engineer Salary Kazakhstan," *SalaryExpert.com*. [Online]. Available: https://www.salaryexpert.com/salary/job/process-engineer/kazakhstan. [Accessed: Apr. 19, 2025].

[110] G. Towler and R. K. Sinnott, "Chapter 9 – Economic Evaluation of Projects," in *Chemical Engineering Design: Principles, Practice and Economics of Plant and Process Design*, 2nd ed.,

Butterworth-Heinemann, 2013, pp. 399–430. [Online]. Available: https://doi.org/10.1016/B978-0-08-096659-5.00009-2.

Appendix

Appendix is available upon request.